AN ANALYTICAL STUDY OF BOUNDARY LAYERS IN MAGNETO-GAS DYNAMICS

by

Lawrence Joseph Coulter

A Dissertation Submitted to the Faculty of the

DEPARTMENT OF AEROSPACE AND MECHANICAL ENGINEERING

In Partial Fulfillment of the Requirements
For the Degree of

DOCTOR OF PHILOSOPHY

In the Graduate College

THE UNIVERSITY OF ARIZONA

1 9 6 5

THE UNIVERSITY OF ARIZONA

GRADUATE COLLEGE

I hereby recommend that this dissertation prepared under my direction by Lawrence Joseph Coulter

entitled An Analytical Study of Boundary Layers in Magneto-Gas Dynamics

be accepted as fulfilling the dissertation requirement of the degree of Doctor of Philosophy

E K Parks — 2/16/65

Dissertation Director — Date

After inspection of the dissertation, the following members of the Final Examination Committee concur in its approval and recommend its acceptance:*

E K Parks	2/16/65
R. E. Peterson	2/16/65
Willard F. Rogers	2/16/65
Ivan Berg	2/16/65
Jay E. Treat, Jr.	2/16/65
Edward A. Hanning	2/16/65

*This approval and acceptance is contingent on the candidate's adequate performance and defense of this dissertation at the final oral examination. The inclusion of this sheet bound into the library copy of the dissertation is evidence of satisfactory performance at the final examination.

STATEMENT BY AUTHOR

This dissertation has been submitted in partial fulfillment of requirements for an advanced degree at The University of Arizona and is deposited in the University Library to be made available to borrowers under rules of the Library.

Brief quotations from this dissertation are allowable without special permission, provided that accurate acknowledgment of source is made. Requests for permission for extended quotation from or reproduction of this manuscript in whole or in part may be granted by the head of the major department or the Dean of the Graduate College when in his judgment the proposed use of the material is in the interests of scholarship. In all other instances, however, permission must be obtained from the author.

SIGNED: Laurence J. Coulter

ACKNOWLEDGMENTS

I wish to thank Dr. Edwin K. Parks for his interest and suggestions in this work. The many hours of discussion with him on this subject have proven most helpful. Also I wish to thank the National Science Foundation for the fellowships which have made my studies possible.

TABLE OF CONTENTS

TABLE OF CONTENTS--Continued

LIST OF ILLUSTRATIONS

ABSTRACT

The general equations necessary to describe the laminar, compressible, boundary layer flow are obtained for a body with a transverse magnetic field. Numerical results are obtained for the case of an adiabatic flat plate by the use of a digital computer. Throughout the analysis, it is assumed that the magnetic effects are limited to the flow region located between the body surface and the bow shock. For the flat plate, the Mach line originating at the leading edge is assumed to be the equivalent of the bow shock. The various properties of the fluid are allowed to vary with temperature. The fluid is assumed to be a continuum.

It is found that a significant increase in the various boundary layer thicknesses and in the total drag occurs for reasonable values of the Hartmann number. A decrease occurs in the local skin friction coefficient. Also, it is found that separation can occur due to the induced pressure gradient.

For the adiabatic flat plate, approximate expressions for the velocity boundary layer thickness and the location of the separation point are obtained by fitting curves to the computer solutions.

CHAPTER I

INTRODUCTION

History

The prefix magneto- on hydrodynamics, aerodynamics, gas dynamics, etc., implies that the subject is concerned with the action of electromagnetic fields on the flow fields of electrically conducting fluids. Although electromagnetic theory and fluid dynamics have each had a great impact on the technological advances over the years, the combination has been of relatively limited interest to engineers until the last decade. Until flows with a significant electrical conductivity were practical, only a few engineering applications were made.

The earliest engineering application in the field of magneto-fluid dynamics is the electromagnetic pump, invented in 1918 by Hartmann (8).[1] However, the first publication on magneto-fluid dynamics dates from 1937, when Hartmann and Lazarus (9) described experiments on the action of magnetic fields on the flow field of mercury.

Interest in magneto-fluid dynamics resulted from the experiments of Hartmann and Lazarus (9), who were able

---

1. Numbers in parenthesis refer to the list of References.

to force a turbulent flow of mercury to return to laminar flow by the application of a magnetic field. About ten years ago, Stuart (24) and Lock (17) calculated the effect of a magnetic field on the critical Reynolds number for an incompressible, electrically conducting fluid flowing between parallel plates. The results of their analysis show that there is a much greater effect on the critical Reynolds number by a magnetic field normal to the flow than by a parallel magnetic field. The normal field produces a retarding force in the primary flow direction, and hence a stabilizing influence is developed.

The concept of a boundary layer and the development of the associated theory began in 1904 with the presentation of a paper by L. Prandtl and his students. However, not until the 1930's did boundary layer theory take its place as an aid to the engineer. Modern investigations have been characterized by a close relationship between theory and experiment.

The electromagnetic pump was the first of many energy conversion applications to be considered on an engineering basis. With the advent of high velocity re-entry vehicles the possibility of controlling the drag and heat transfer by the application of magneto-gas dynamical principles to the ionized air in front of the vehicle required the development of "new" methods of flow analysis, which combined the two divisions of physics; gas dynamics

and electrodynamics. The theory of magneto-gas dynamical motion may be formulated as a strictly theoretical problem, independent of its physical applications. Although many interesting situations may be developed from strictly theoretical analysis, it becomes necessary to determine those situations which are realizable in a practical engineering sense.

If, as in most cases considered, the electrical conductivity is considered to be very large and the currents are attenuated slowly, the magnetic field appears to be frozen in the medium for long periods of time. If the medium is in hydrodynamical motion, then the field is deformed with the medium. The magnetic flux through any surface formed in the medium will, of course, be retained. The medium in the magnetic field becomes anisotropic. Motion parallel to the field is not changed by the field and will remain as in ordinary hydrodynamics. However, motion normal to the field causes deformation of the field with an accompanying transformation of the kinetic energy of the fluid into electromagnetic energy, or vice versa. Such transformations cause a number of new effects which are not encountered in ordinary hydrodynamics.

Boundary Layer Literature

The majority of papers which fall under the heading of magneto-fluid dynamics are not directly concerned with

boundary layer problems. Since the boundary layer problem is the principal subject in this dissertation, this review of magneto-fluid dynamics will be restricted to those problems which are concerned with boundary layer effects. The early work of such people as Batchelor, Bullard, Chandrasekhar and Thompson have greatly contributed to the general knowledge of magneto-fluid dynamics.

Rossow (20), under the assumption of a linear dependence of conductivity on velocity, has calculated the boundary layer effects for an incompressible, electrically conducting fluid flowing over a flat plate in the presence of a magnetic field. Rossow's analysis shows that the application of a magnetic field normal to a flat plate, while reducing the viscous forces at the surface, causes an increase in total drag.

Braum (3) has considered the possibility of reducing stagnation point heat transfer rates on blunt bodies at hypersonic speeds by means of magnetic fields. Neglecting compressibility effects very near the stagnation point, and under the assumption that the Prandtl number is equal to one, Braum concludes that it does not seem practicable to significantly reduce the aerodynamic heating load on such bodies by magnetic techniques unless the electrical conductivity of air is artificially enhanced when the free stream Mach number is less than ten.

In conclusion, prior treatments of boundary layer analysis in magneto-fluid dynamics have assumed that the flow was incompressible. While this assumption yields reasonably valid results for stagnation regions, compressibility effects are important away from the stagnation region and can not be neglected in boundary layer regions.

Present Investigation

The object of this study is to present an analysis of boundary layer flow when acted upon by a magnetic field.

In order to obtain general equations of motion, the variation of such parameters as electrical conductivity, thermal conductivity, viscosity, etc., with temperature are considered.

In order to determine the influence parameters in boundary layer flow, the equations of motion are reduced by an order of magnitude analysis.

A digital computer was used to obtain numerical solutions for the case of an adiabatic flat plate. Investigation includes boundary layer growth, velocity and temperature profiles, viscous drag and total drag for laminar flow. Also, the possibility of separation is analyzed. Variations of the Reynolds number, the Hartmann number, the Prandtl number and the Mach number are considered.

Finally, the results were compared to those of ordinary boundary layer analysis to determine the influence

of the magnetic parameters. The applicability and usefulness of such conclusions to high velocity satellite reentry problems and to energy conversion devices make the investigation of current interest.

CHAPTER II

IONIZED GASES

Introduction to Ionized Gases

Magneto-fluid dynamics assumes an electrically conducting medium which may be a liquid or an ionized gas. There is a trend towards indicating the medium under discussion by considering the subject as magneto-hydrodynamics when assuming a liquid, and magneto-gas dynamics when assuming an ionized gas. This study will concern only magneto-gas dynamics. If the ionized gas can be regarded as a continuum, both types of media can be treated under a common theory.

Figure 2.1 shows the composition of air at very high temperatures for standard sea level density. It can be seen that dissociation of neutral molecules of nitrogen and oxygen becomes significant near 3000°C and ionization of nitrogen atoms becomes significant around 10,000°C and oxygen, 15,000°C. For lower densities ionization will begin at lower temperatures (not shown).

Dissociation occurs when the energy of the internal degrees of freedom becomes sufficient to overcome the binding energy holding the atoms together. Equilibrium dissociation is achieved when the rate of dissociation of

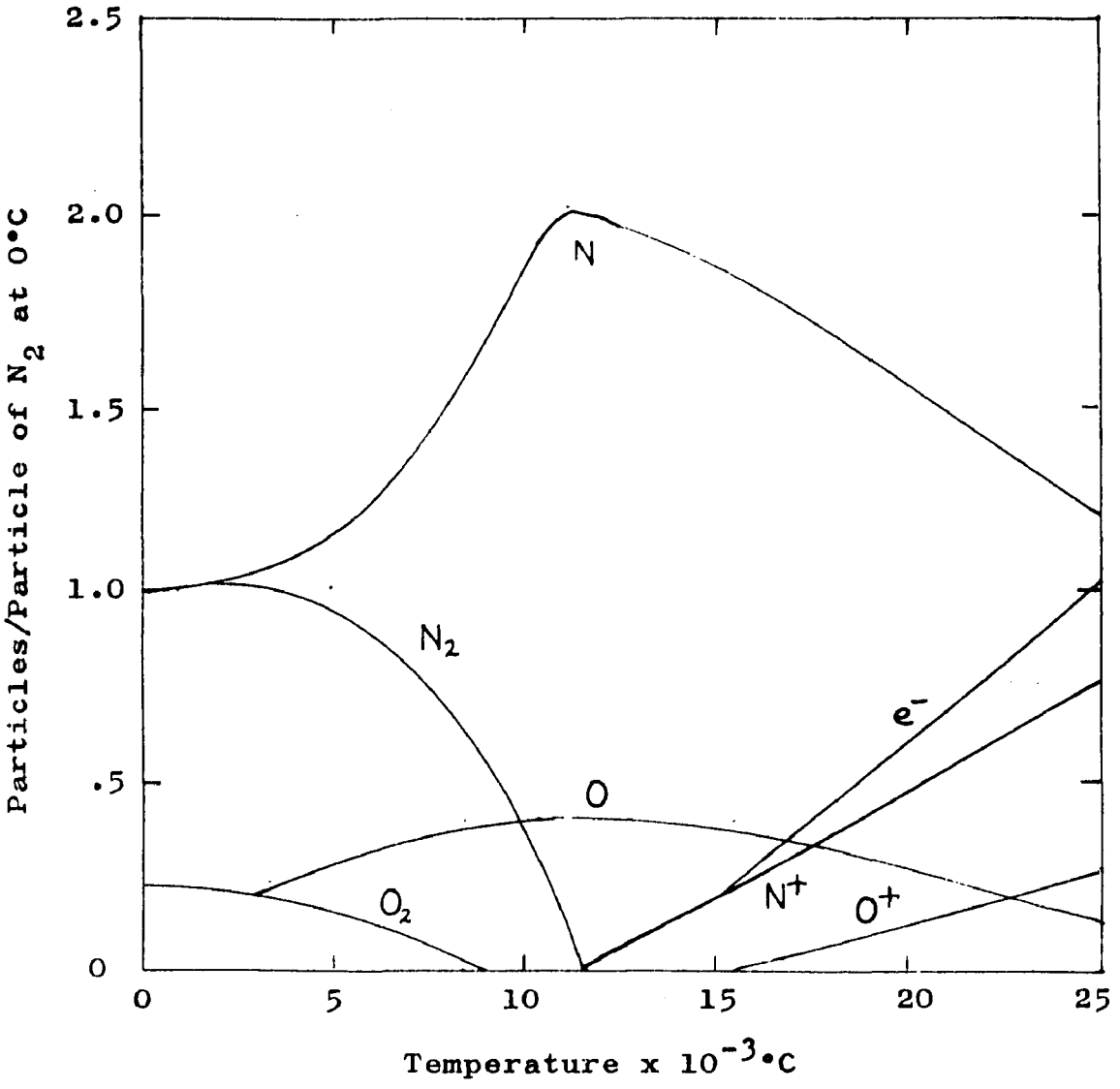

Figure 2.1 Composition of Air at Atmospheric Density

After Hilsenrath and Klein (11)

the molecules into atoms is equal to the rate of recombination of atoms into molecules. The rate of dissociation or ionization will be proportional, as a first approximation, to the number of collisions occuring between molecules and atoms which have sufficient energy to cause dissociation or ionization. There is a characteristic relaxation time which depends on the time necessary for the energy that is added to the translational degrees of freedom of a molecule or atom by collision to become distributed among all of the degrees of freedom of the molecule or atom. For example, although a molecule receives sufficient energy for dissociation by collision, the molecule does not dissociate until the energy of the vibrational degree of freedom reaches a sufficient value to overcome the binding forces holding the atoms of the molecule together. Measurements on argon by Lin, Resler and Kantrowitz (16) have shown that argon reaches ionization equilibrium in the order of ten microseconds following maximum luminosity for temperatures greater than 11,000°K.

Degree of Ionization

The degree of ionization of a gas in equilibrium may be predicted from a thermodynamic argument. Saha (21), in 1920, first presented a relation for a gas whose atoms are ionized by losing only one electron, i.e., a singly ionized gas. Saha has assumed that a singly ionized gas

can be regarded as being in a state of dynamic equilibrium represented by a completely reversible reaction of the form,

$$A = A^{+} + e - Q_i, \tag{2.1}$$

where A represents a neutral atom, A^{+} a singly ionized atom, e the electron removed from the atom, and Q_i the ionization energy. Based on this equation Saha applied Nernst's equation to air in ionization equilibrium, resulting in the expression,

$$\frac{x^2}{1-x^2} P = 3.16 \times 10^{-7} T^{5/2} \exp(-Q_i/kT), \tag{2.2}$$

where P = total pressure, atoms,

T = temperature, deg. K,

Q_i = ionization energy, ergs,

x = degree of ionization, dimensionless,

k = Boltzman's constant = 1.380×10^{-16} ergs/deg.,

which has come to be known as the Saha equation. In many practical problems the degree of ionization is sufficiently small to justify the simplifying substitution of unity for $1-x^2$ in the equation 2.2.

Von Engel (5) states that there is ample evidence obtained indirectly from investigations on arcs which supports the view that the thermodynamic treatment of Saha is justified. Lin, Resler, and Kantrowitz (16) use the Saha

equation in their studies of ionized argon, and show that the experimental results agree with theory when the assumption of equilibrium is valid.

The Ionized Gas Equation of State

The equilibrium composition and thermodynamic properties of air to 24,000°K have been calculated by Gilmore (6) and Hilsenrath and Klein (11). The calculation by Gilmore includes the composition, pressure, energy and entropy of dry air at eleven temperatures between 1,000 and 24,000°K, and eight densities between 10^{-6} and 10 times standard sea level density. The analysis by Gilmore (6) assumes an ideal gas mixture in chemical equilibrium, including dissociation and ionization.

Kantrowitz and Petschek (13) have considered a generalized classification of magneto-gas dynamics by plotting electron density vs temperature at constant pressure for the equilibrium state. Figure 2.2 shows part of their data. Kantrowitz and Petschek (13) assume that electrons exhibit appreciable relativistic effects above 10^{10}K and quantum effects become important in the region labeled degenerate gases.

It has been stated earlier that magneto-hydrodynamics and magneto-gas dynamics may be treated by a common theory if the gas can be regarded as a continuum. In gas dynamics it is usual to consider the Knudsen number, the

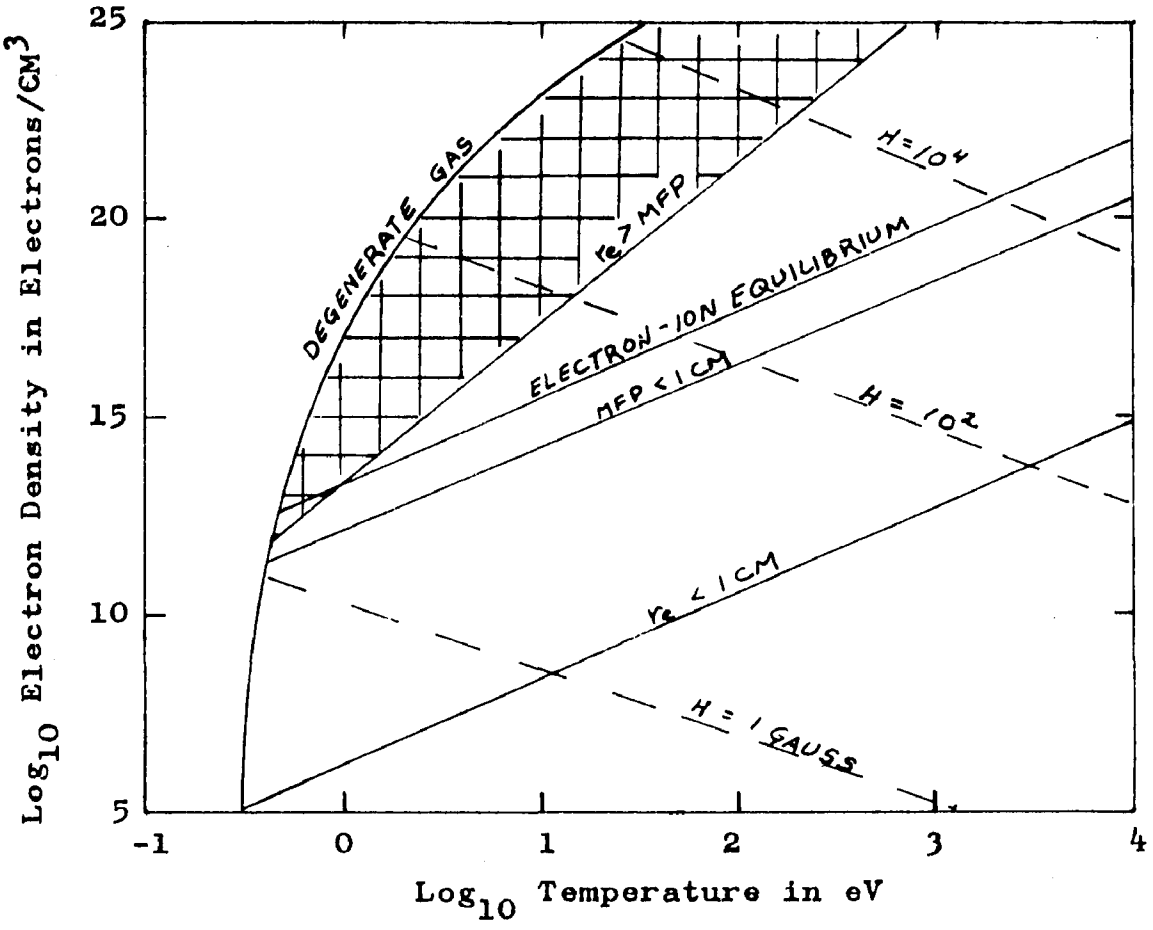

Figure 2.2 Electron Equilibrium Diagram

$$P = 2n_e kT$$

After Kantrowitz and Petschek (13)

ratio of the mean free path to the characteristic length of the system, much less than unity as defining a continuum region. However, for magneto-gas dynamics, other criteria become important. The assumption of a continuum for ionized gases requires that the free electron motion be dominated by interaction with other particles, i.e., the collision frequency is sufficiently high to prevent free spiraling of electrons. It has been found that free spiraling of electrons is prevented when the electron Larmor radius, r_e, is greater than the mean free path of electrons (see Gubanov and Pushkarev, ref. 7). The electron Larmor radius is defined as

$$r_e = \frac{m_e c}{e\ H} \left(\frac{8kT}{\pi m_e}\right)^{1/2}, \text{ CM} \qquad (2.3)$$

where H = magnetic intensity, gauss

c = velocity of light, 2.998×10^{10} cm/sec

m_e = electron mass, 9.107×10^{-28} gm

e = electron charge, 4.803×10^{-10} esu

T = temperature, °K

k = Boltzmann's constant, 1.380×10^{-16} ergs/°K

and gives the radii of the helices described by electrons moving in a magnetic field.

In the cross-hatched region of Figure 2.2 the magnetic field effect and other effects are small compared with collision effects, and the distribution function for

particles will be close to a Maxwellian velocity distribution as in a neutral gas. In this region, where $r_e >$ mfp, the electrons will drift through the ionized gas in a manner analogous to the diffusion of neutral molecules, and the assumptions indicated in the following section on the electrical conductivity are valid. This region is the region of prime importance in this paper.

The "perfect gas" equation of state for a dissociated or ionized gas in equilibrium,

$$P = \frac{\rho RT}{M} \sum_i n_i, \qquad (2.4)$$

where R = universal gas constant,
8.31436×10^7 ergs/mole-°K,
P = pressure, dynes/cm^2,
T = temperature, °K,
ρ = density, gm/cm^3,
n_i = particles per atom,
M = atomic weight,

is used by Gilmore (6) in calculating the composition of air to 24,000°K. In using equation 2.4, M is the atomic weight, 14.549 for air, since the n_i are defined as particles per (air) atom. The chemical composition will be essentially constant for a slightly ionized gas and a highly ionized gas, and equation 2.4 takes on an even simpler form since the terms n_i will be constant.

An equation of state for ionized hydrogen has been developed by Williamson (27), as

$$P = \frac{\rho kT}{1/2H}\left[1 - 0.0140\left(\frac{\rho/100}{(T/10^7)^3}\right)^{1/2}\right], \qquad (2.5)$$

where H = proton mass, 1.673×10^{-24} gm.

Kaeppeler and Baumann (12) give the following equation of state applicable to any degree of ionization, any gas, and any density.

$$\frac{P}{kT\sum_i N_i} = 1 - \frac{e^2 r}{6\epsilon kT}\frac{\sum N_i x_i f(ra_i)}{\sum N_i} \qquad (2.6)$$

where $r = \left(4\pi e^2 \sum_i N_i x_i^2/kT\right)^{1/2}$,

$f(ra_i) = 1 - \frac{263}{4} ra_i + \ldots$,

e = electron charge (4.802×10^{-10} e.s.u.),

N_i = density, ions/cm^3,

x_i = valence,

a_i = ion radius, cm,

k = Boltzmann's constant (1.380×10^{-16} ergs/°K),

T = temperature, °K,

ϵ = permittivity, esu.

Williamson's equation of state for ionized hydrogen, equation 2.5, is contained in the equation of state by Kaeppeler and Baumann (12), equation 2.6, as a special case.

Hilsenrath and Klein have shown that the correction to the "perfect gas" equation of state is less than four percent for ionized gas when the density is less than standard sea level. Since the physical region of interest for this problem is the region of low density (10^{-1} atmospheres or less) it appears reasonable to use the "perfect gas" equation of state.

Electrical Conductivity

The electrical conductivity of ionized gases depends on the diffusivity of electrons in the gas. At low degrees of ionization, the diffusivity depends primarily on the cross section of electron-atom collisions. At high degrees of ionization, the diffusion is limited by the long range Coulomb forces.

For a slightly ionized gas Lin, Resler and Kantrowitz (16) developed the following expression from measurements of electrical conductivity:

$$\sigma_a = 0.532e^2 \, x / (m_e kT)^{1/2} q_a, \ \frac{\text{Mhos}}{\text{CM}} , \qquad (2.7)$$

where q_a = electron-atom cross section,

e = electron charge, e.s.u.,

m_e = electron mass,

x = degree of ionization (equation 2.2),

k = Boltzmann's constant,

T = temperature, °K.

For a highly ionized gas, Spitzer and Harm (23) developed the expression

$$\sigma_d = 0.591(kT)^{3/2}/m_e^{1/2}e^2\ln(h/b_o), \ \frac{\text{Mhos}}{\text{CM}} \qquad (2.8)$$

where e = electron charge, e.s.u.,

h = Debye shielding distance,

$= \left(kT/8\pi N_e e^2\right)^{1/2}$, cm,

b_o = impact parameter $= e^2/3kT$, cm,

N_e = electron density, electrons/cm^3.

Lin, et al, found good agreement for all ranges of ionization levels if these two conductances (equations 2.8 and 2.7) were treated as conductances in series. Thus

$$\sigma = \left[\frac{1.88(m_e kT)^{1/2} q_a}{xe^2} + \frac{1.69 m_e^{1/2} e^2 \ln(h/b_o)}{(kT)^{3/2}}\right]^{-1}. \qquad (2.9)$$

While the first term in equation 2.9 appears to vary inversely with the temperature, the degree of ionization, equation 2.2, is a strong function of the temperature and hence, the electrical conductivity increases with an increase in temperature.

Recent test data reported by von Karman (15) shows that the electric conductivity varies inversely as M^2 in the region behind a shock wave for Mach numbers ranging from about six to eighteen and inversely as M^3 for Mach numbers ranging from eighteen to thirty. This appears to

be consistent with equation 2.9 in that the Mach number is inversely proportional to the one-half power of the temperature.

Viscosity

The general formulae for the first approximation to the viscosity and thermal conductivity in the absence of external forces have been evaluated by S. Chapman (4) for a completely ionized gas and by L. L. Moore (19) for moderate temperatures. The coefficient of viscosity can be expressed as

$$\frac{\mu}{\mu_i} = \left(\frac{T}{T_i}\right)^N \qquad (2.10)$$

where μ = coefficient of viscosity,

T = temperature,

and $(\ )_i$ = reference state.

The value of exponent, N, varies with the temperature. For moderate temperatures, Moore predicted the value of N to range from one half to three halves. At extreme temperatures where ionization is essentially complete, Chapman found the value of N to be five halves.

$$\begin{aligned} N &= 1/2 \text{ for moderately low temperatures,} \\ &= 3/2 \text{ for moderately high temperatures,} \\ &= 5/2 \text{ for extremely high temperatures.} \end{aligned} \qquad (2.11)$$

If N is treated as a linearly varying function of the degree of ionization, that is,

$$N = 1/2 + 3/2\ x \tag{2.12}$$

the error in predicting the coefficient of viscosity was less than four percent when the calculated value was compared with those presented by Moore (19) and Chapman (4). Thus, for this analysis, it is assumed that

$$\frac{\mu}{\mu_i} = \left(\frac{T}{T_i}\right)^{1/2 + 3/2\ x} \tag{2.13}$$

Thermal Conductivity

The first order variation of the coefficient of thermal conductions closely parallels the variation of the coefficient of viscosity. The variation can be expressed as

$$\frac{\Lambda}{\Lambda_i} = \left(\frac{T}{T_i}\right)^{N} \tag{2.14}$$

where Λ = coefficient of thermal conduction,

T = temperature,

and $(\ )_i$ = reference state.

As with the coefficient of viscosity, the exponent, N, ranges from one half to five halves. For this analysis, it is assumed that

$$\frac{\Lambda}{\Lambda_i} = \left(\frac{T}{T_i}\right)^{1/2 + 3/2\ x} \tag{2.15}$$

Prandtl Number

The Prandtl number is defined as

$$Pr = \frac{\mu c_p}{\Lambda} \tag{2.16}$$

The viscosity and thermal conductivity for a gas have been presented in previous sections. The specific heat of a highly ionized gas was approximated by Chapman (4) as

$$c_p = \frac{3}{2}\frac{k}{m_i} \tag{2.17}$$

where k = Boltzman's constant,

and m_i = ion mass.

The specific heat for a monatomic gas (a dissociated gas) can be approximated by

$$c_p = \frac{5}{2}\frac{k}{m} \tag{2.18}$$

where k = Boltzman's constant,

and m = atomic mass.

von Kármán (15) demonstrated that, in the area of magneto-aeronautics, the variation of the Prandtl number can be based on the amount of ionization. von Kármán obtained the empirical expression

$$\frac{Pr}{Pr_\infty} = 1 - x \tag{2.19}$$

where $Pr_\infty = 0.721$

and x = degree of ionization (equation 2.2),

for temperatures less than 5×10^5°K. Equation 2.19 is used in this analysis.

Region of Interest

While the general region of interest is the one of a continuum, the cross-hatched region in Figure 2.2, specific interest for this analysis was restricted to the region of aerodynamic flows. Mach numbers in the neighborhood of fifty can produce stagnation temperatures of approximately 55,000°K or 5 eV. An additional vertical line can be added to Figure 2.2 to further restrict the area of interest (not shown).

In this area, two effects, that of radiation and species diffusion, can be neglected. Several authors have recently considered the effects of radiation with respect to the flow variables. Energy radiated per unit volume for the region of interest has been shown by B. Kivel (von Kármán, 14) to have a maximum value of about 10 watt-sec/cm^3. The kinetic energy of a unit volume entering the boundary layer will be converted to thermal energy when the fluid velocity is decreased. The kinetic energy is a function of the initial velocity and ranges from approximately 200 to 1000 watt-sec/cm^3 in the region of interest. For maximum radiation and minimum energy the maximum error due to neglecting the radiation term in the energy balance is on the order of 3%.

Braum (3) discussed the contribution of species diffusion for various regions of interest. In his analysis, a distance over which diffusion would be significant was defined. For the case of the stagnation boundary layers, that is the case of the maximum thermal gradients relevant to flow analysis, the distance for which an excess charge density resulting from species diffusion was shown to be on the order of 5 times the mean free path of the gas. Thus on a macroscopic scale the effect of diffusion is not significant.

CHAPTER III

EQUATIONS OF MOTION

Electromagnetic Equations

A tabulation of the macroscopic equations of electromagnetic theory is given below for convenient reference.

$$\overline{D} = \epsilon_e \overline{E} \tag{3.1}$$

$$\overline{B} = \mu_e \overline{H} \tag{3.2}$$

$$\nabla \cdot \overline{D} = \rho_c \tag{3.3}$$

$$\nabla \cdot \overline{B} = 0 \tag{3.4}$$

$$\nabla \times \overline{E} = -\partial \overline{B}/\partial t \tag{3.5}$$

$$\nabla \times \overline{B} = \mu_e (\overline{J} + \partial \overline{D}/\partial t) \tag{3.6}$$

In addition, Ohm's Law may be written as

$$\overline{J} = \sigma(\overline{E} + \overline{q} \times \overline{B}) + \rho_e \overline{q} \tag{3.7}$$

Continuity Equation

The continuity equation for continuum magneto-gas dynamics requires no additional electromagnetic terms and is the same as that for a neutral gas.

$$\frac{\partial \rho}{\partial t} + \nabla\cdot(\rho\bar{q}) = 0 \qquad (3.8)$$

Momentum Equations

The momentum equations consist of the usual Navier-Stokes equations plus electromagnetic force terms due to the motion of a conductive fluid through magnetic lines of force and due to excess charge density in the fluid. The latter effect, that of forces due to the excess charge density, will be neglected.

$$\rho\frac{D\bar{q}}{Dt} = -\nabla P + \nabla\cdot(\mu\nabla\bar{q}) + \frac{\nabla}{3}(\mu\nabla\cdot\bar{q}) + \bar{J}\times\bar{B} \qquad (3.9)$$

Energy Equation

The energy equation for continuum magneto-gas dynamics consists of the usual terms as written for a neutral gas plus the heating effects due to the electromagnetic actions and the energy stored in the field.

$$\rho\frac{Dh}{Dt} = \frac{DP}{Dt} + \nabla\cdot(k\nabla T) + \Phi + \bar{q}\cdot\bar{J}\times\bar{B} \qquad (3.10)$$

where

$$\Phi = (2\mu+\mu_1)(\nabla\cdot\bar{q})^2 + \mu\left[\left(\frac{\partial v}{\partial x}+\frac{\partial u}{\partial y}\right)^2 + \left(\frac{\partial w}{\partial y}+\frac{\partial v}{\partial z}\right)^2 + \left(\frac{\partial u}{\partial z}+\frac{\partial w}{\partial x}\right)^2\right] \qquad (3.11)$$

In order to obtain a unique solution to the problem, it is necessary to have the same number of equations as dependent variables.

In a three dimensional problem the fifteen dependent variables are three components of the magnetic flux, three components of the electric flux, three components of the electric current, three components of the fluid velocity, the fluid pressure, the fluid density, and the fluid temperature. The corresponding fifteen independent equations are six scalar equations obtained from Maxwell's equations, three scalar equations obtained from Ohm's Law, the equation of continuity, the three scalar momentum equations, the energy rate equation, and the equation of state. In addition, an equation is necessary for each fluid property which is allowed to vary, i.e., the coefficients of viscosity and electrical conductivity.

Certain other variables are used in this paper for convenience but can be expressed in terms of the dependent variables listed above, i.e., the Mach number and the Reynolds number. With the set of fifteen equations involving fifteen dependent variables together with appropriate boundary conditions the problem is mathematically determinant.

CHAPTER IV

MODEL

Statement of Model

The problem under consideration is the solution for the flow parameters for flow of an ionized gas over a flat plate with a constant magnetic field applied perpendicular to the plate.

The following assumptions are made:

1. The fluid is treated as a continuum.
2. The free stream velocity is parallel to the plate.
3. The flow in all regions is in a steady state.
4. The flow near the plate (i.e., $y < \delta$) is a laminar, two-dimensional flow.
5. The flow outside the boundary layer is inviscid.
6. The applied electric field is zero.
7. The magneto-gas dynamical effects are confined to a region bounded by the plate and a Mach wave originating at the leading edge of the plate.

The last assumption is arbitrary. In the case of an actual body the bow shock wave would be the logical outer boundary for magneto-gas dynamical effects. As the body thickness becomes infinitesimally small, i.e., a flat plate, the bow

shock wave is replaced by the Mach line. Figure 4.1 represents the configuration for study.

General Flow Analysis

It was first shown by Prandtl that the Navier-Stokes equations can be simplified in regions where rapid changes of variables occur essentially in a direction normal to the main flow. When x is taken in the direction of the main flow and the argument restricted to two dimensional steady flow, the governing equations can be simplified by neglecting certain smaller magnitude terms resulting from the smallness of v and the small rate of change of all quantities in the x direction as compared to their rate of change in the y direction. The complete analysis leading to the simplified equations for two dimensional steady flow has been treated in Schlichting (22, chapter XIV) with the exception of the electromagnetic terms. Only the electromagnetic terms will be considered in detail here.

Reduced Equations of Motion

The continuity equation, equation 3.8, remains unchanged from that given by Schlichting (22) for steady flow

$$\frac{\partial}{\partial x}(\rho u) + \frac{\partial}{\partial y}(\rho v) = 0. \qquad (4.1)$$

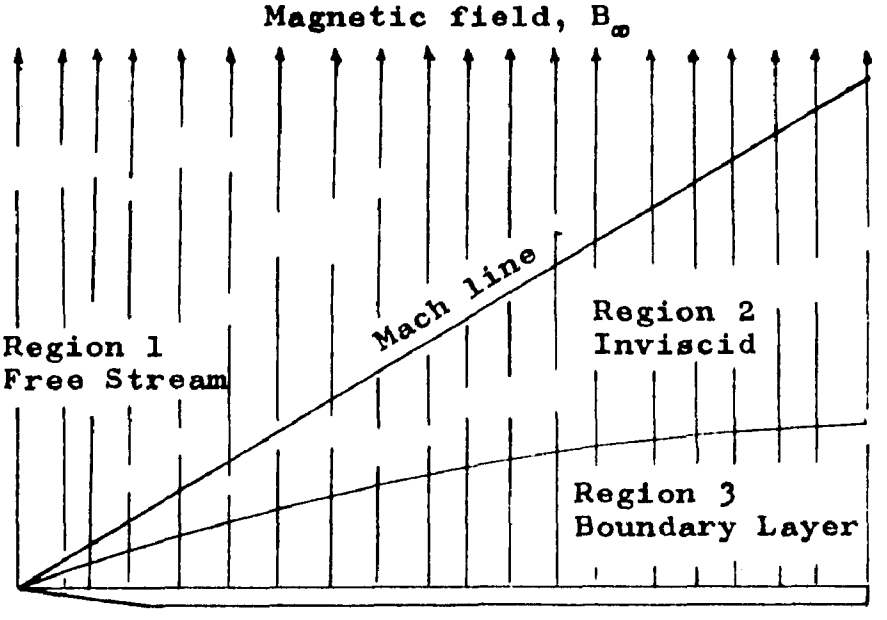

Figure 4.1 Problem Model

Region 1: Free Stream Flow with no magnetic effects

Region 2: Inviscid Flow with magnetic effects

Region 3: Boundary Layer Flow

The x-momentum equation from equation 3.9 is

$$\rho(u\frac{\partial u}{\partial x} + v\frac{\partial u}{\partial y}) = -\frac{\partial p}{\partial x} + \bar{i}\cdot\bar{J}x\bar{B} + \frac{\partial}{\partial y}(\mu\frac{\partial u}{\partial y}). \qquad (4.2)$$

Using the assumption that the magnetic field is applied only in the y direction and is constant in magnitude

$$\bar{J}x\bar{B} = -\sigma B^2 u\bar{i} + \text{higher order terms}. \qquad (4.3)$$

The higher order terms are discussed later. Thus the x-momentum equation becomes

$$\rho(u\frac{\partial u}{\partial x} + v\frac{\partial u}{\partial y}) = -\frac{\partial P}{\partial x} - \sigma B^2 u + \frac{\partial}{\partial y}(\mu\frac{\partial u}{\partial y}) + \text{higher order terms}. \qquad (4.4)$$

Likewise the y-momentum becomes

$$\rho(u\frac{\partial v}{\partial x} + v\frac{\partial v}{\partial y}) = -\frac{\partial P}{\partial y} + \frac{\partial}{\partial x}(\mu\frac{\partial v}{\partial x}) + \Psi \qquad (4.5)$$

where Ψ is the term resulting from $\bar{J}$ x $\bar{B}$. It is desired to withhold further analysis of Ψ until later.

The energy equation, equation 3.10, can be expressed as

$$\rho(u\frac{\partial h}{\partial x} + v\frac{\partial h}{\partial y}) = u\frac{\partial P}{\partial x} + \Phi + \frac{\partial}{\partial y}(k\frac{\partial T}{\partial y}) + \bar{q}\cdot(\bar{J}x\bar{B}). \qquad (4.6)$$

Under the assumption in the Statement of Model, the magnetic contribution can be expressed as

$$\bar{q}\cdot(\bar{J}x\bar{B}) = \sigma B^2 u^2 + \text{higher order terms}. \qquad (4.7)$$

Substituting equation 4.7 into equation 4.6, the final expression for the energy rate equation becomes

$$\rho\left(u\frac{\partial h}{\partial x} + v\frac{\partial h}{\partial y}\right) = u\frac{\partial P}{\partial x} + \mu\left(\frac{\partial u}{\partial y}\right)^2 + \frac{\partial}{\partial y}\left(k\frac{\partial T}{\partial y}\right) + \sigma B^2 u^2$$

$$+ \text{higher order terms} \qquad (4.8)$$

Order of Magnitude Analysis

Non-dimensional variables are defined in the following manner:

$$u^* = u/u \ , \ v^* = v/u \ ,$$

$$x^* = x/L, \ y^* = y/L,$$

$$T^* = T/(T_w - T_\infty),$$

$$P^* = P/\rho_\infty U_\infty^2, \ \rho^* = \rho/\rho_\infty \qquad (4.9)$$

The x-momentum equation, equation 4.4, with the above substitutions can be written in the following form,

$$\rho^*\left(u^*\frac{\partial u^*}{\partial x^*} + v^*\frac{\partial u^*}{\partial y^*}\right) = -\frac{\partial P^*}{\partial x^*} - \frac{\sigma B_\infty^2 L}{\rho_\infty U_\infty} u^*$$

$$+ \frac{\mu_\infty}{\rho_\infty U_\infty L}\ \frac{\partial}{\partial y^*}\left(\mu^*\frac{\partial u^*}{\partial y^*}\right) \qquad (4.10)$$

The coefficients of the velocity gradient and the velocity appearing on the right hand side of equation 4.10 are recognized as the reciprocal of the Reynolds number and the

ratio of the square of the Hartmann number to the Reynolds number respectively.

$$\text{Reynolds Number, } Re \equiv \rho uL/\mu. \tag{4.11}$$

$$\text{Hartmann Number, } Ha \equiv (\sigma B^2 L^2/\mu)^{1/2}. \tag{4.12}$$

The ratio of the Hartmann number squared to the Reynolds number is often called the magnetic influence parameter,

$$\lambda \equiv \frac{Ha^2}{Re} \equiv \frac{\sigma B^2 L}{\rho u} . \tag{4.13}$$

On the same physical basis as reference 22 one can assign the order unity, O(1), to the magnitude of u^* and x^* and the order δ/L, $O(\delta/L)$, to the magnitude of v^* and y^*.

The x-momentum equation is then observed to be the following

$$u^*\frac{\partial u^*}{\partial x^*} + v^*\frac{\partial u^*}{\partial y^*} = \frac{-1}{\rho^*}\left[\frac{\partial P^*}{\partial x^*} + \lambda u^* - \frac{1}{Re}\frac{\partial}{\partial y^*}\left(\mu^*\frac{\partial u^*}{\partial y^*}\right)\right]$$

$$O(1) \quad O(1) \quad O(1) \; ? \quad ? \; O(1) \; ? \quad O(L^2/\delta^2) \tag{4.14}$$

Since the left hand side of equation 4.14 is of order unity, terms on the right hand side of the equation must be of order unity or larger to have a significant influence on the solution.

The following statements can now be made:

$$\text{for viscous influence} \qquad O(Re) = O(L^2/\delta^2); \tag{4.15}$$

for pressure gradient influence $O(\partial P^*/\partial x^*) = O(1)$; (4.16)

for electromagnetic influence $O(\lambda) = O(1)$. (4.17)

Similarly, the y-momentum equation, equation 4.5, may be written as

$$u^*\frac{\partial v^*}{\partial x^*} + v^*\frac{\partial v^*}{\partial y^*} = -\frac{1}{\rho^*}\left[\frac{\partial P}{\partial y^*} - \frac{\mu^*}{Re}\frac{\partial^2 v^*}{\partial y^{*2}} + \frac{\Psi L}{\rho U_\infty^2}\right]$$

$$O(\delta/L) \quad O(\delta/L) \quad O(1) \quad ? \quad O(\delta/L) \quad ? \qquad (4.18)$$

Under the assumption that the applied field is

$$\overline{B}_\infty = \overline{B}_\infty \overline{j}. \qquad (4.19)$$

the induced field, $\overline{b}$, may be found from Maxwell's equation 3.6 and Ohm's Law 3.7.

$$\nabla \times \overline{b} = \mu_e \sigma \overline{q} \times \overline{B}_\infty \qquad (4.20)$$

The induced field in the x-direction, b_x, is related to the applied field and the velocity components by the equation,

$$\frac{\partial b_x}{\partial y} = -\sigma \mu_e u B_\infty. \qquad (4.21)$$

Thus

$$b_x = -\int_0^y \sigma \mu_e u B_\infty dy. \qquad (4.22)$$

Hence, the magnetic force term ($\overline{J} \times \overline{B}$ form) becomes

$$\sigma(\overline{q}x(\overline{B}_\infty+\overline{b})) \times (\overline{B}_\infty+\overline{b}) = \overline{i}\sigma(-B_\infty^2 u+vB_\infty b_x) + \overline{j}\sigma(-vb_x^2+uB_\infty b_x). \quad (4.23)$$

Thus

$$\overline{i}\cdot(\overline{J} \times \overline{B}) = -\sigma B_\infty^2 u + O(\delta^2/L^2), \quad (4.24)$$

and

$$\overline{j}\cdot(\overline{J} \times \overline{B}) = \sigma b_x u B_\infty + O(\delta^3/L^3). \quad (4.25)$$

From equation 4.22, $O(b_x)$ is no larger than an order of δ/L. Returning to equation 4.5,

$$\Psi = \sigma b_x B_\infty u, \quad (4.26)$$

and

$$\frac{\Psi L}{\rho_\infty U_\infty^2} = \lambda u^* b_x^* \quad (4.27)$$

which is no larger than order δ/L. Using this in equation 4.18, and comparing the various terms in the equation, it may be observed that the pressure gradient in the y-direction, $\partial P^*/\partial y^*$, is of $O(\delta/L)$. Since $\partial P^*/\partial x^*$ is of an order larger than $\partial P^*/\partial y^*$, we may assume that the pressure varies only along the x-axis and treat $\partial P^*/\partial x^*$ as a total derivative. When the pressure variation is thus restricted, the pressure in the boundary layer region may be determined by the boundary conditions at the outer edge and hence the number of unknowns is reduced by one. This fact allows us

to reduce the number of equations by one. Since the y-momentum equation is an order of magnitude smaller than the other equations, it is chosen to be the one which is not considered.

Similarly the energy equation in dimensionless form may be written as

$$u^* \frac{\partial T^*}{\partial x^*} + v^* \frac{\partial T^*}{\partial y^*} = \frac{E}{\rho^*}\left[\lambda u^{*2} + \frac{1}{Re} \Phi + \frac{dP^*}{dx^*} u^* + \frac{1}{PrRe} \frac{\partial^2 T^*}{\partial y^{*2}} \right]$$

$$O(1) \quad O(1) \quad \frac{?}{O(1)} \quad O(1) \quad O(1) \quad O(1) \quad ? \; O(L^2/\delta_T^2) \tag{4.28}$$

where δ_T is the thermal boundary layer thickness and

$$E = u_\infty^2 / c_p (T_w - T_\infty), \tag{4.29}$$

$$Pr = \mu \, c_p / k. \tag{4.30}$$

For convenience μ, c_p, and k have been considered to be constant within one order of magnitude in equation 4.28. The following statements may now be made:

for heat generation influence $O(E) = O(1)$; (4.31)

for conductive influence $O(1/PrRe) = O(\delta_T^2/L^2)$. (4.32)

In the case of a gas, the Prandtl number is nearly unity. Comparing equations 4.32 and 4.15, it is observed

that the thermal boundary layer is of the same order of thickness as the velocity boundary layer,

$$O(\delta_T) = O(\delta). \tag{4.33}$$

Discussion of Model

The model can now be written in terms of applicable equations for the three regions of flow.

Region 1. Free stream

The various variables from this region (i.e., M_∞, T_∞, etc.) are used as boundary conditions.

Region 2. Inviscid flow

The various variables are assumed to be acted upon by the magnetic field. However, the flow is assumed to be one dimensional, without shear and with negligible thermal conduction. The use of these assumptions allows further reduction of the equations of motion. The resulting equations of motion for Region 2# are

1. Continuity

$$\frac{\partial}{\partial x}(\rho_o u_o) = 0, \tag{4.34}$$

2. Momentum

$$\rho_o \frac{\partial u_o}{\partial x} = -\frac{dp_o}{dx} - \sigma_o B_\infty^2 u_o, \tag{4.35}$$

A subscript $_o$ will be used to denote the flow variables in Region 2.

3. Energy

$$\rho_o u_o \frac{\partial h_o}{\partial x} = u_o \frac{dp_o}{dx} + \sigma_o B^2 u_o^2. \tag{4.36}$$

Region 3. Boundary layer flow

The flow is forced to match the inviscid solution along a curve $y = \delta(x)$ where $\delta(x)$ is the velocity boundary layer thickness.

The resulting equations of motion are

1. Continuity

$$\frac{\partial}{\partial x}(\rho u) + \frac{\partial}{\partial y}(\rho v) = 0, \tag{4.37}$$

2. Momentum

$$\rho(u\frac{\partial u}{\partial x} + v\frac{\partial u}{\partial y}) = -\frac{dp}{dx} - \sigma B_\infty^2 u + \frac{\partial}{\partial y}(\mu\frac{\partial u}{\partial y}), \tag{4.38}$$

3. Energy

$$\rho(u\frac{\partial h}{\partial x} + v\frac{\partial h}{\partial y}) = u\frac{dp}{dx} + \sigma B^2 u^2 + \Phi + \frac{\partial}{\partial y}(k\frac{\partial T}{\partial y}) \tag{4.39}$$

where $\Phi = \mu(\frac{\partial u}{\partial y})^2$.

The electron equilibrium diagram, Figure 2.2, contains a cross-hatched region where ionized gases may be represented as continuous fluids. This region is the prime region of interest, both experimentally and theoretically, since it is the region of physical applications. Theoretically, it is the region in which the macroscopic equations of fluid dynamics and electromagnetic theory are valid.

Experimentally, ionized gases, which fall in the region where the continuum assumption is valid, are naturally easier to obtain because of the proximity of this region to the region of a continuous neutral gas. Lysen and Serovy (18) give an extensive review of the types of problems that can be treated, based on the assumption that the fluid may be represented as a continuum.

The phenomena of viscous interaction in the flow over a flat plate has been discussed at great length in the literature, e.g., Schlichting (22). For flow of a real fluid, i.e., one with viscosity, the flow is retarded primarily in the vicinity of the body surface. This region, called the boundary layer, is observable. While many definitions of the boundary layer thickness are used, the most physical definition is the one based on the mass flux defect, called the displacement thickness, δ^*. The inviscid flow outside the boundary layer sees a body which is represented by the physical body plus the displacement thickness. The effective change in the shape of the body gives rise to the body shape factor, β. The velocity boundary layer thickness, δ, the thickness for which the local velocity is equal to the free stream velocity, has been previously defined.

It will be assumed that the velocity and thermal boundary layer thicknesses are equal. While this is true only if the Prandtl number is unity, it is considered a

first approximation when the Prandtl number is of order unity. Bogdonoff and Hammitt (2) concluded that the error introduced by this assumption may be as great as 50% for the thermal boundary layer thickness but is insignificant for the boundary layer thicknesses related to momentum.

CHAPTER V

INVISCID FLOW SOLUTIONS

Equations of Motion

Based upon the assumptions made in Chapters II (Ionized Gas) and IV (Model), the equations of motion for region 2 may be written as

1. Continuity

$$\frac{d}{dx}(\rho_\bullet u_\bullet) = 0 \tag{5.1}$$

2. Momentum

$$\rho_\bullet u_\bullet \frac{du_\bullet}{dx} = - \frac{dp_\bullet}{dx} - \sigma_\bullet B_\infty^2 u_\bullet \tag{5.2}$$

and

3. Energy

$$\rho_\bullet u_\bullet \frac{dh_\bullet}{dx} = u_\bullet \frac{dp_\bullet}{dx} + \sigma_\bullet B_\infty^2 u_\bullet^2. \tag{5.3}$$

Density and Pressure

The equation of continuity may be integrated directly. Applying the boundary conditions from the free stream flow, we have

$$\rho_\bullet u_\bullet = \rho_\infty u_\infty. \tag{5.4}$$

Solving for the density ratio

$$\frac{\rho_*}{\rho_\infty} = \frac{u_\infty}{u_*} \cdot \tag{5.5}$$

From Chapter II we may write the pressure ratio as

$$\frac{P_*}{P_\infty} = \frac{\rho_* h_*}{\rho_\infty h_\infty} \cdot \tag{5.6}$$

Substituting for the density yields

$$\frac{P_*}{P_\infty} = \frac{u_\infty}{u_*} \frac{h_*}{h_\infty} \cdot \tag{5.7}$$

Enthalpy

To obtain an enthalpy profile for the inviscid region it is necessary to solve the energy equation 5.3. Differentiating equation 5.7 with respect to a dimensionless length, x^*, yields

$$\frac{dP_*}{dx^*} = P_\infty \left[\frac{u_\infty}{u_*} \frac{1}{h_\infty} \frac{dh_*}{dx^*} - \frac{h_*}{h_\infty} \frac{u_\infty}{u_*^2} \frac{du_*}{dx^*} \right] , \tag{5.8}$$

and with use of equation 5.3,

$$\frac{dh_*}{dx^*} = \frac{\gamma-1}{\gamma} \left[\frac{dh_*}{dx^*} - \frac{h_*}{u_*} \frac{du_*}{dx^*} \right] + \lambda_* u_*^2 \tag{5.9}$$

or

$$\frac{1}{h_*} \frac{dh_*}{dx^*} = - \frac{\gamma-1}{u_*} \frac{du_*}{dx^*} + \gamma(\gamma-1)\lambda_* M_*^2 \tag{5.10}$$

From the section on electrical conductivity we may write

$$\lambda_* = \lambda_\infty M_\infty^2 / M_*^2. \tag{5.11}$$

Then, integrating equation 5.10 yields

$$\ln\left(\frac{h_*}{h_\infty}\right) = -\ln\left(\frac{u_*}{u}\right)^{\gamma-1} + \gamma(\gamma-1)\lambda_\infty M_\infty^2 x^* \tag{5.12}$$

or

$$\frac{h_*}{h_\infty} = \left(\frac{u_*}{u}\right)^{1-\gamma} \exp\left[\gamma(\gamma-1)\lambda_\infty M_\infty^2 \frac{x}{L}\right]. \tag{5.13}$$

Velocity

By using equation 5.10 in connection with 5.8 we may solve the momentum equation 5.2 for the velocity profile. Writing equation 5.2 in a non-dimensional form gives

$$\frac{d(u_*/u_\infty)}{dx^*} = -\frac{1}{\rho_\infty u_\infty^2}\frac{dp_*}{dx^*} - \lambda_* \frac{u_*}{u_\infty}. \tag{5.14}$$

However, combining equation 5.8 and 5.10 results in

$$\frac{dp_*}{dx^*} = \gamma P_\infty \frac{h_*}{h_\infty}\frac{u_\infty}{u_*}\left[(\gamma-1)\lambda_\infty M_\infty^2 - \frac{u_\infty}{u_*}\frac{d(u_*/u_\infty)}{dx^*}\right]. \tag{5.15}$$

Substituting 5.15 into 5.14 and solving for $d(u_*/u_\infty)/dx^*$ gives

$$\frac{d(u_*/u_\infty)}{dx^*} = -\frac{\gamma\lambda_\infty M_\infty^2 u_*}{(M_*^2-1)\,u_\infty}. \tag{5.16}$$

In the following section it is shown that M_* may be expressed as a function of x^* only (see equation 5.23). Hence, for the purpose of computer integration, we may write

$$\frac{u_*}{u_\infty} = \exp\left(-\delta \lambda_\infty M_\infty^2 \int_0^{x^*} \frac{dx^*}{M_*^2 - 1}\right). \tag{5.17}$$

Mach Number

The logarithmic differential of the square of the Mach number is

$$\frac{dM^2}{M^2} = \frac{du^2}{u^2} - \frac{da^2}{a^2} . \tag{5.18}$$

However,

$$\frac{da^2}{a^2} = \frac{dh}{h} , \tag{5.19}$$

and

$$\frac{du^2}{u^2} = 2\frac{du}{u} . \tag{5.20}$$

Thus

$$\frac{dM_*^2}{M_*^2} = 2\frac{du_*}{u_*} - \frac{dh_*}{h_*} . \tag{5.21}$$

Combining equations 5.21, 5.10, and 5.16 yields,

$$\frac{dM_*^2}{M_*^2} = -\frac{2\gamma\lambda_* M_*^2}{M_*^2-1}\left[1+\frac{\gamma-1}{2}M_*^2\right]dx^* . \qquad (5.22)$$

Using the expression for λ_*, given in equation 5.11, we can integrate equation 5.22 to obtain

$$\left[\frac{1+\frac{\gamma-1}{2}M_*^2}{1+\frac{\gamma-1}{2}M_\infty^2}\right]^{\frac{\gamma+1}{\gamma-1}}\frac{M_\infty^2}{M_*^2} = \exp\left[-2\gamma\lambda_\infty M_\infty^2\frac{x}{L}\right] . \qquad (5.23)$$

Summary of Inviscid Flow

In this chapter the following relationships have been established:

$$\frac{\rho_*}{\rho_\infty} = \frac{u_\infty}{u_*} ; \qquad (5.24)$$

$$\frac{P_*}{P_\infty} = \frac{u_\infty}{u_*}\frac{h_*}{h_\infty} ; \qquad (5.25)$$

$$\frac{h_*}{h_\infty} = \left(\frac{u_*}{u_\infty}\right)^{1-\gamma}\exp\left[\gamma(\gamma-1)\lambda_\infty M_\infty^2\frac{x}{L}\right] ; \qquad (5.26)$$

$$\frac{u_*}{u_\infty} = \exp\left[-\gamma\lambda_\infty M_\infty^2\int_0^{x^*}\frac{dx^*}{M_*^2-1}\right] ; \qquad (5.27)$$

$$\left[\frac{1+\frac{\gamma-1}{2}M_*^2}{1+\frac{\gamma-1}{2}M_\infty^2}\right]^{\frac{\gamma+1}{\gamma-1}}\frac{M_\infty^2}{M_*^2} = \exp\left[-2\gamma\lambda_\infty M_\infty^2\frac{x}{L}\right] . \qquad (5.28)$$

These five relationships will be used in the following chapter as the boundary conditions for the outer edge of the viscous boundary layer flow of Region 3. Numerical examples are presented in Chapter VII.

CHAPTER VI

PROBLEM SOLUTION

General Method

The method of solution of the flow variables is one of obtaining a finite difference equation for the boundary layer thickness which may then be solved by computer techniques. The momentum and energy equations will be put in integral forms. Before these two equations can be further developed it is necessary to establish a velocity profile. After the method of Pohlhausen, a polynomial will be used to represent the velocity profile. While this method satisfies the boundary conditions, it does not satisfy the momentum equation throughout the boundary layer region. However, since the integral form of the momentum equation is used, knowledge of the exact solution for the velocity profile is not necessary. Schlichting (22) compared Pohlhausen's solution with the so called "exact" solutions for the ordinary case and found the error to be very small.

The outer boundary conditions for the boundary layer region will be based on the inviscid flow solutions. It will be assumed that the only pressure gradient is that induced by the magnetic field.

The resulting analysis yields a differential equation for the boundary layer thickness coupled to other equations involving the outer boundary conditions and wall conditions. A solution is then obtained by use of a digital computer.

Velocity Profile

The ratio of u to u_e is assumed to be a polynomial function of η.

$$f(\eta) = \frac{u}{u_e} = a\eta + b\eta^2 + c\eta^3 + d\eta^4 + e, \tag{6.1}$$

where $\eta = \frac{1}{\delta_1} \int_0^y \frac{\rho}{\rho_e} dy$; $\delta_1 = \int_0^\delta \frac{\rho}{\rho_e} dy$;

and a, b, c, d, and e may be functions of x.

The boundary conditions are

$$y = 0 \qquad u = v = 0 \qquad \text{or } f(0) = 0; \tag{6.2}$$

$$y = \delta_1 \qquad u = u_e \qquad \text{or } f(1) = 1; \tag{6.3}$$

$$y = \delta_1 \qquad \frac{\partial u}{\partial y} = 0 \qquad \text{or } f'(1) = 0; \tag{6.4}$$

$$y = \delta_1 \qquad \frac{\partial^2 u}{\partial y^2} = 0 \qquad \text{or } f''(1) = 0. \tag{6.5}$$

By considering the momentum equation at the wall, a fifth "boundary condition" may be determined.

$$\mu_w \left(\frac{\partial^2 u}{\partial y^2}\right)_{wall} = \frac{dP}{dx} . \tag{6.6}$$

Equation 6.6, with the use of equation 4.35, can be written as

$$f''(0) = -\beta \tag{6.7}$$

where

$$\beta = \frac{\rho_\bullet}{\rho_w} Re_\bullet \frac{\delta_1^2}{L^2} \left[\frac{1}{u_\bullet} \frac{du_\bullet}{dx/L} + \lambda_\bullet\right] . \tag{6.8}$$

β is the body shape factor discussed previously.

Since the velocity at the wall must vanish, no constant term may appear in equation 6.1 and hence, e must be zero. Solving for the other coefficients appearing in equation 6.1:

$$a = 2 + \beta/6, \tag{6.9}$$

$$b = -\beta/2, \tag{6.10}$$

$$c = -2 + \beta/2, \tag{6.11}$$

$$d = 1 - \beta/6. \tag{6.12}$$

Finally, the velocity profile can be written in the following manner:

$$\frac{u}{u_\bullet} = f(\eta) = F(\eta) + \beta G(\eta), \tag{6.13}$$

where

$$F(\eta) = 1 - (1 - \eta)^3(1 + \eta), \tag{6.14}$$

$$G(\eta) = (1 - \eta)^3/6, \tag{6.15}$$

and β is defined in equation 6.8.

It is observed that the velocity profile reduces to that given in Schlichting (22) for the case of no magnetic field, $\lambda = 0$.

Momentum Integral

The momentum equation 4.38 can be solved for the shear term and integrated with respect to y.

$$\int_o^\delta \frac{\partial}{\partial y}\left(\mu\frac{\partial u}{\partial y}\right)dy = \int_o^\delta \left(\rho u\frac{\partial u}{\partial y} + \rho v\frac{\partial u}{\partial y} + \sigma B^2 u + \frac{dP}{dx}\right)dy \tag{6.16}$$

Consider the term on the left.

$$\int_o^\delta \frac{\partial}{\partial y}\left(\mu\frac{\partial u}{\partial y}\right)dy = \left[\mu\frac{\partial u}{\partial y}\right]_o^\delta = \mu_o\frac{\partial u}{\partial y}\bigg|_\delta - \mu_w\left(\frac{\partial u}{\partial y}\right)_w \tag{6.17}$$

Since $\left(\frac{\partial u}{\partial y}\right)_\delta = 0$, this term reduces to

$$-\mu_w\left(\frac{\partial u}{\partial y}\right)_w = -\tau_w . \tag{6.18}$$

From the continuity equation 4.37

$$\rho v = -\int_o^y \frac{\partial}{\partial x}(\rho u)dy . \tag{6.19}$$

Then

$$\int_o^\delta \left(\rho v\frac{\partial u}{\partial y}\right)dy = -\int_o^\delta \left[\frac{\partial u}{\partial y}\int_o^y \frac{\partial}{\partial x}(\rho u)dy\right]dy \tag{6.20}$$

Integrating by parts yields

$$\int_0^{\delta} (\rho v \frac{\partial u}{\partial y}) dy = - \int_0^{\delta} \left[u_{\bullet} \frac{\partial \rho u}{\partial x} - u \frac{\partial \rho u}{\partial x} \right] dy. \tag{6.21}$$

It has previously been shown that

$$\frac{dP}{dx} = \frac{dP_{\bullet}}{dx} = - \rho_{\bullet} u_{\bullet} \frac{du_{\bullet}}{dx} - \sigma_{\bullet} B_{\infty}^2 u_{\bullet} . \tag{6.22}$$

Substituting equations 6.18, 6.21, and 6.22 into equation 6.16 gives

$$\tau_w = \int_0^{\delta} \left[u_{\bullet} \frac{\partial \rho u}{\partial x} - u \frac{\partial \rho u}{\partial x} - \rho u \frac{\partial u}{\partial x} + \rho_{\bullet} u_{\bullet} \frac{du_{\bullet}}{dx} \right.$$

$$\left. + \sigma_{\bullet} B_{\infty}^2 u_{\bullet} - \sigma B_{\infty}^2 u \right] dy . \tag{6.23}$$

It is now possible to rearrange the terms in equation 6.23 to arrive at the following relationship,

$$\frac{d\theta}{dx} + \frac{\theta}{u_{\bullet}} \frac{du_{\bullet}}{dx} (2 + \frac{\delta^*}{\theta} - M_{\bullet}^2) + \frac{\lambda_{\bullet} \delta_{\sigma}}{L} = \frac{\tau_w}{\rho_{\bullet} u_{\bullet}^2} \tag{6.24}$$

where

$$\theta = \int_0^{\delta} \frac{\rho u}{\rho_{\bullet} u_{\bullet}} (1 - \frac{u}{u_{\bullet}}) dy, \tag{6.25}$$

$$\delta^* = \int_0^{\delta} (1 - \frac{\rho u}{\rho_{\bullet} u_{\bullet}}) dy, \tag{6.26}$$

and

$$\delta_{\sigma} = \int_0^{\delta} (1 - \frac{\sigma u}{\sigma_{\bullet} u_{\bullet}}) dy. \tag{6.27}$$

The definition appearing in equation 6.27 might be considered as an electrical conduction thickness.

It may be observed that if the magnetic field is zero, equation 6.24 reduces to the ordinary equation as presented in Schlichting (22, Chapter XV).

Energy Integral

In a manner similar to that used for the momentum integral, the energy equation can be placed in an integral form. The energy equation 4.39 can be written in the following manner

$$\int_o^\delta \mu \left(\frac{\partial u}{\partial y}\right)^2 dy + \int_o^\delta \frac{\partial}{\partial y}\left(k\frac{\partial T}{\partial y}\right) dy = \int_o^\delta \Big[\rho u \frac{\partial h}{\partial x} + \rho v \frac{\partial h}{\partial y} - u\frac{dP}{dx} - \sigma B^2 u^2 \Big] dy. \tag{6.28}$$

Substituting as before for ρv and dP/dx and using the definition of the Prandtl number, the energy integral can be written as

$$\frac{d}{dx}(\rho_\bullet u_\bullet h_\bullet \theta_H) + \rho_\bullet u_\bullet^2 \frac{du_\bullet}{dx}\theta_H + \sigma_\bullet B_\infty^2 u_\bullet^2 \theta_\sigma = \left[\frac{\mu}{Pr}\frac{\partial h}{\partial y}\right]_w + \int_o^\delta \mu \left(\frac{\partial u}{\partial y}\right)^2 dy, \tag{6.29}$$

where

$$\theta_H = \int_o^\delta \frac{\rho u}{\rho_\bullet u_\bullet}\left(\frac{h}{h_\bullet} - 1\right) dy \tag{6.30}$$

$$\theta_\sigma = \int_0^{\sigma} \frac{u}{u_\bullet} \left(1 - \frac{\sigma u}{\sigma_\bullet u_\bullet}\right) dy. \tag{6.31}$$

As before, equation 6.29 reduces to the solution given by Schlichting (22) if the magnetic field is set equal to zero and if the wall is adiabatic.

Boundary Layer Thickness

The various boundary layer thicknesses can be found by using the momentum integral equation, equation 6.24, and the energy integral equation, equation 6.29, together with the inviscid solutions obtained in Chapter V. The momentum integral as previously developed is

$$\frac{d\theta}{dx} + \frac{\theta}{u_\bullet}\frac{du_\bullet}{dx}\left(2 + \frac{\delta^*}{\theta} - M_\bullet^2\right) = -\frac{\lambda_\theta \delta_\sigma}{L} + \frac{\tau_w}{\rho_\bullet u_\bullet^2} \tag{6.32}$$

From Chapter II and the fact that $\partial p/\partial y = 0$, the density can be expressed as a function of the enthalpy in the boundary layer.

$$\frac{\rho}{\rho_\bullet} = \frac{h_\bullet}{h}. \tag{6.33}$$

The shear stress, equation 6.18, with the use of the velocity profile, equation 6.13, can be written as

$$\frac{\tau_w}{\rho_\bullet u_\bullet^2} = \frac{\mu_w}{\mu_\bullet}\frac{\rho_w}{\rho_\bullet}\frac{1}{Re_\bullet}\frac{L}{\delta_1} f'(0). \tag{6.34}$$

Substituting for $f''(0)$ yields

$$\frac{\tau_w}{\rho_\bullet u_\bullet^2} = \frac{\mu_w}{\mu_\bullet}\frac{\rho_w}{\rho_\bullet}\frac{1}{Re_\bullet}\frac{L}{\delta_1}(2 + \beta/6). \tag{6.35}$$

The following terms may also be evaluated in terms of β with the use of the velocity profile.

$$\frac{\theta}{\delta_1} = \int_0^1 \frac{u}{u_\bullet}(1 - \frac{u}{u_\bullet})d\eta$$

$$= \frac{37}{315} - \frac{\beta}{945} - \frac{\beta^2}{9072} \tag{6.36}$$

$$\int_0^1 \frac{u}{u_\bullet}d\eta = \frac{7}{10} + \beta/120 \tag{6.37}$$

Using equations 6.35, 6.36, and 6.37, equation 6.32 may be written in the form

$$\frac{\theta}{\delta_1}\frac{\delta_1}{L}\frac{d\delta_1}{dx} + \frac{\delta_1^2}{L^2}\left[\frac{\theta}{\delta_1}\frac{1}{u_\bullet}\frac{du_\bullet}{dx}(2-M_\bullet^2) - \frac{1}{u_\bullet}\frac{du_\bullet}{dx}(\frac{7}{10} + \frac{\beta}{120})\right]$$

$$+ \frac{\delta_1^2}{L^2}\int_0^1\left[\frac{1}{u_\bullet}\frac{du_\bullet}{dx/L} + \lambda_\bullet(1 - \frac{u\sigma}{\sigma_\bullet u_\bullet})\right]\frac{\rho_\bullet}{\rho}d\eta = \frac{\mu_w}{\mu_\bullet}\frac{\rho_w}{\rho_\bullet}\frac{(2+\beta/6)}{Re_\bullet}. \tag{6.38}$$

With the definitions

$$z = \delta_1^2/L^2, \tag{6.39}$$

$$K' = \frac{1}{u_\bullet}\frac{du_\bullet}{dx/L}, \tag{6.40}$$

and $$K = K' + \lambda_\bullet, \tag{6.41}$$

equation 6.38 becomes

$$\frac{dz}{dx/L} = -\frac{z}{2}\frac{\delta_1}{\theta}\left[\frac{\theta}{\delta_1}K'(2-M_\infty^2)-K'\left(\frac{7}{10}+\frac{\beta}{120}\right)+I\right]$$

$$+\frac{\mu_w}{\mu_\infty}\frac{\rho_w}{\rho_\infty}\frac{(1+\beta/12)}{Re_\infty\theta/\delta_1} \qquad (6.42)$$

where

$$I = \int_0^1\left[K'+\lambda_\infty\left(1-\frac{u\sigma}{\sigma_\infty u_\infty}\right)\right]\frac{\rho_\infty}{\rho}d\eta. \qquad (6.43)$$

Once an expression for the density or the enthalpy is obtained, equation 6.43 can be evaluated. Equation 6.42 is an ordinary first order differential equation with variable coefficients which, at least numerically, can be integrated.

Enthalpy Profile

At this point of the analysis it is useful to restrict the problem to the adiabatic wall. Although this prevents an analysis of the heat transfer at the wall, it allows the dominating factor in the boundary layer flow to be that due to the magnetic field.

For an adiabatic wall

$$\left(\frac{\partial T}{\partial y}\right)_w = 0. \qquad (6.44)$$

With this boundary condition and with the Prandtl number equal to unity, the enthalpy may be shown to be a function of the velocity component in the x direction.

Assume that the enthalpy may be written as

$$h = a + cu^2. \tag{6.45}$$

Since the gradient at the wall is zero, equation 6.44, a linear component need not be considered. The derivatives of h are

$$\frac{\partial h}{\partial x} = 2cuu_x, \tag{6.46}$$

$$\frac{\partial h}{\partial y} = 2cuu_y, \tag{6.47}$$

and

$$\frac{\partial^2 h}{\partial y^2} = 2cuu_{yy} + 2cu_y^2. \tag{6.48}$$

Substituting the above expressions into the energy equation 4.39 yields

$$2cu(\rho uu_x+\rho vu_y) = u\frac{dP}{dx} + \sigma B_\infty^2 u^2+\mu u_y^2 + 2c\mu(u_y^2+uu_{yy}). \tag{6.49}$$

If the momentum equation 4.38 is multiplied by 2cu and subtracted from the above equation we obtain

$$0 = u(\frac{dP}{dx} +\sigma B_\infty^2 u)(1+2c)+\mu(2c+1)u_y^2. \tag{6.50}$$

Since the modified energy equation must be valid at the wall

$$c = -1/2. \tag{6.51}$$

Thus

$$h = a - u^2/2. \tag{6.52}$$

Applying the boundary condition,

$$h = h_\bullet \text{ at } \eta = 1, \tag{6.53}$$

$$\frac{h}{h_\bullet} = 1 + \frac{\gamma-1}{2} M_\bullet^2 \left(1 - \frac{u^2}{u_\bullet^2}\right) \tag{6.54}$$

In the case $Pr \neq 1$, a temperature recovery factor, r, must be introduced. While the factor is a function of the flow conditions, it has been shown by several authors (references 14 and 22) that the recovery factor is approximately equal to the square root of the Prandtl number.

$$\frac{h}{h_\bullet} = 1 + \frac{\gamma-1}{2} M_\bullet^2 Pr^{1/2} \left(1 - \frac{u^2}{u_\bullet^2}\right) \tag{6.55}$$

for an adiabatic wall.

The preceding method will not yield a solution if the adiabatic wall restriction is released. Appendix A contains the more general development showing that the temperature (enthalpy) is a function of u alone only for the adiabatic wall. In the general case the energy equation is non-linear and is coupled with equation 6.42.

Drag Coefficients

The total drag on a body is comprised of two contributions. The first is due to the viscous shear, τ_w,

at the surface of the plate. The second is due to reaction between the flow and the magnetic field.

The local shear force has been defined as

$$\tau_w = (\mu \frac{\partial u}{\partial y})_w . \tag{6.56}$$

Then

$$c_f = \frac{1}{1/2 \rho_\infty u_\infty^2} (\mu \frac{\partial u}{\partial y})_w . \tag{6.57}$$

In analyzing the effects of the magnetic field the ratio of the magnetic skin friction coefficient to that of the ordinary case will be used.

The total drag coefficient is defined as

$$c_d = \int_0^\infty \frac{\rho u}{\rho_\infty u_\infty} (1 - \frac{u}{u_\infty}) dy. \tag{6.58}$$

It may be assumed that the effects of the magnetic field are negligible outside the area defined by the body surface and the bow shock wave for an arbitrary body. Since the Mach line for a flat plate has somewhat of an equivalence to a bow shock wave for an arbitrary body, the contribution due to the magnetic influence will be restricted by the Mach line. Hence the upper limit for the integral appearing in equation 6.58 is taken to be

$$y = L \tan(\sin^{-1}(1/M_\infty)). \tag{6.59}$$

Collected Equations

Thus far a set of coupled equations has been developed for the adiabatic flat plate. Since closed-form solutions are not obtainable, a digital computer was used to obtain numerical solutions. The purpose of this section is to present in final form the primary equations used in writing the computer program. Because the symbolism used in Fortran languages is limited and somewhat unique, the symbolism used in this section will be consistent with the preceding chapters and not with the computer program appearing in Appendix B. The program is self-contained and confusion in symbolism has been avoided as much as possible by the use of comment cards.

In Chapter II, it was found that the coefficients of viscosity and thermal conductivity vary as h^n where n is a function of the ionization level and ranges from 1/2 to 5/2. It is assumed that the variation of n is linear with the percentage of ionization.

The momentum integral, equation 6.42, may be written in the form

$$\frac{dz}{dx} + P(x)z = Q(x), \tag{6.60}$$

where

$$P(x) = \frac{1}{2}\frac{\rho_1}{\theta}\left[\frac{\theta}{\rho_1}K'(2-M_e^2) - K'\left(\frac{7}{10} + \frac{\beta}{120}\right) + I\right] \tag{6.61}$$

and

$$Q(x) = \left(\frac{h_w}{h_\bullet}\right)^{n-1} \frac{1}{Re_\bullet} \frac{\delta_1}{\theta}(1+\beta/12). \tag{6.62}$$

Since P(x) and Q(x) are in parametric form, it is not possible to obtain an integrating factor. Instead, the Runge-Kutta method, Reference 10, for a finite difference equation will be used. To the third power of dx the finite difference equation for equation 6.60 may be written as

$$z(x+\Delta x) = z(x) + (A_1+4A_2+A_3)/6 \tag{6.63}$$

where $$A_1 = [Q(x) - P(x)\cdot z(x)]\Delta x \tag{6.64}$$

$$A_2 = \left\{Q\left(x + \frac{\Delta x}{2}\right) - P\left(x + \frac{\Delta x}{2}\right)\cdot\left[z(x) + \frac{A_1}{2}\right]\right\} \Delta x \tag{6.65}$$

and $$A_3 = \left\{Q(x+\Delta x) - P(x+\Delta x)\cdot[z(x)+2A_1-A_2]\right\} \Delta x. \tag{6.66}$$

The following equations were used in the computer program:

Inviscid Mach number, equation 5.28,

$$\left[\frac{1 + \frac{\gamma-1}{2}M_\bullet^2}{1 + \frac{\gamma-1}{2}M_\infty^2}\right]^{\frac{\gamma+1}{\gamma-1}} \frac{M_\infty^2}{M_\bullet^2} = \exp(-2\gamma M_\infty^2 \lambda_\infty \frac{x}{L}). \tag{6.67}$$

Other inviscid parameters,

$$\frac{du_\bullet/u_\infty}{dx/L} = - \frac{\gamma \lambda_\infty M_\infty^2}{M_\bullet^2-1} u_\bullet/u_\infty; \tag{6.68}$$

$$\frac{h_\bullet}{h_\infty} = \left(\frac{u_\bullet}{u_\infty}\right)^{1-\gamma} \exp\left[\gamma(\gamma-1)\lambda_\infty M_\infty^2 \frac{x}{L}\right]; \tag{6.69}$$

$$\frac{P_e}{P_\infty} = \frac{u_\infty}{u_e}\frac{h_e}{h_\infty} . \tag{6.70}$$

Percent ionization, equation 2.2,

$$\frac{x_i^2}{1-x_i^2} P = 3.16\text{x}10^{-7}T^{5/2}\exp(-Q_i/kT) . \tag{6.71}$$

At this point in the solution the change in the Reynolds number and the Prandtl number and the various gas properties were computed. Also, the enthalpy at the wall was computed.

$$\beta = zKRe_e(h_w/h_e) \tag{6.72}$$

$$\frac{u}{u_e} = F(\eta)+\beta G(\eta) \tag{6.73}$$

$$\frac{h}{h_e} = 1 + \frac{\gamma-1}{2} M_e^2 Pr^{1/2}(1 - \frac{u^2}{u_e^2}) \tag{6.74}$$

At this point the various gas properties were computed for the boundary layer region.

$$\frac{dz}{dx} = -P(x)z+Q(x), \quad (z = \delta_1^2/L^2) \tag{6.75}$$

$$\theta/L = \frac{\theta}{\delta_1}\frac{\delta_1}{L} = \sqrt{z}\, f(\beta) \tag{6.76}$$

$$C_d = \int_0^{x/L \tan(\sin^{-1}\frac{1}{M})} \frac{\rho_e u}{\rho_\infty u_\infty}(1 - \frac{u}{u_\infty})d\eta \tag{6.77}$$

$$C_f = \frac{1}{\rho_e u_e^2}(\mu \frac{\partial u}{\partial y})_w \tag{6.78}$$

$$\frac{T}{T_\bullet} = \frac{hc_{p\bullet}}{h_\bullet c_p} \tag{6.79}$$

The size of the net is variable. Near the leading edge the increment on x/L was chosen as 10^{-6} while after 10% of the plate length was traversed, the increment was increased to 10^{-3}. The former was chosen so as to reduce any error resulting from the necessity of assigning initial values to various parameters such as z and β. The latter increment was chosen so that the truncation error would be greater than or equal to the round off error. The increment on η was chosen as 10^{-2} for the same reason.

In addition to the equations listed above, several consistency checks were incorporated in the program. The two most important ones were the subsonic flow and separation checks. When the inviscid flow reaches sonic velocity, several changes in sign occur. The most obvious change occurs in the exponential appearing in equation 6.67. If the Mach number is less than unity, the exponential becomes positive, as is readily seen from equation 5.22. The condition for separation, the velocity gradient at the wall being zero, implies that separation occurs for $\beta = -12$. Once this value is reached or exceeded negatively, the shear is no longer expressible as a linear function of the velocity gradient. As a result, essentially no equations

developed are valid. The most readily observable case is the momentum integral equation, equation 6.17.

In general, the numerical solutions were obtained by specifying the initial values of z and β, the various gas properties for dissociated air, and the free stream values for the Mach, Reynolds, Prandtl, and Hartmann numbers along with the ratio of specific heats and the plate length. While the information obtainable from the program is essentially unlimited with respect to the problem, certain variables present the flow solution. They are the equations listed in this section together with the two consistency checks discussed.

The flow chart, Figure 6.1, demonstrates the steps which the computer is required to follow. Three basic operations are shown. They are: (1) input/output commands, which cause the computer system to read or write information; (2) block processing, which causes the computer to perform one or more arithmetic operations in sequence; and (3) decisions, which cause the computer to transfer to various block processing areas depending on information which has been previously computed. Appendix B contains the Fortran program written in standard card format for Fortran.

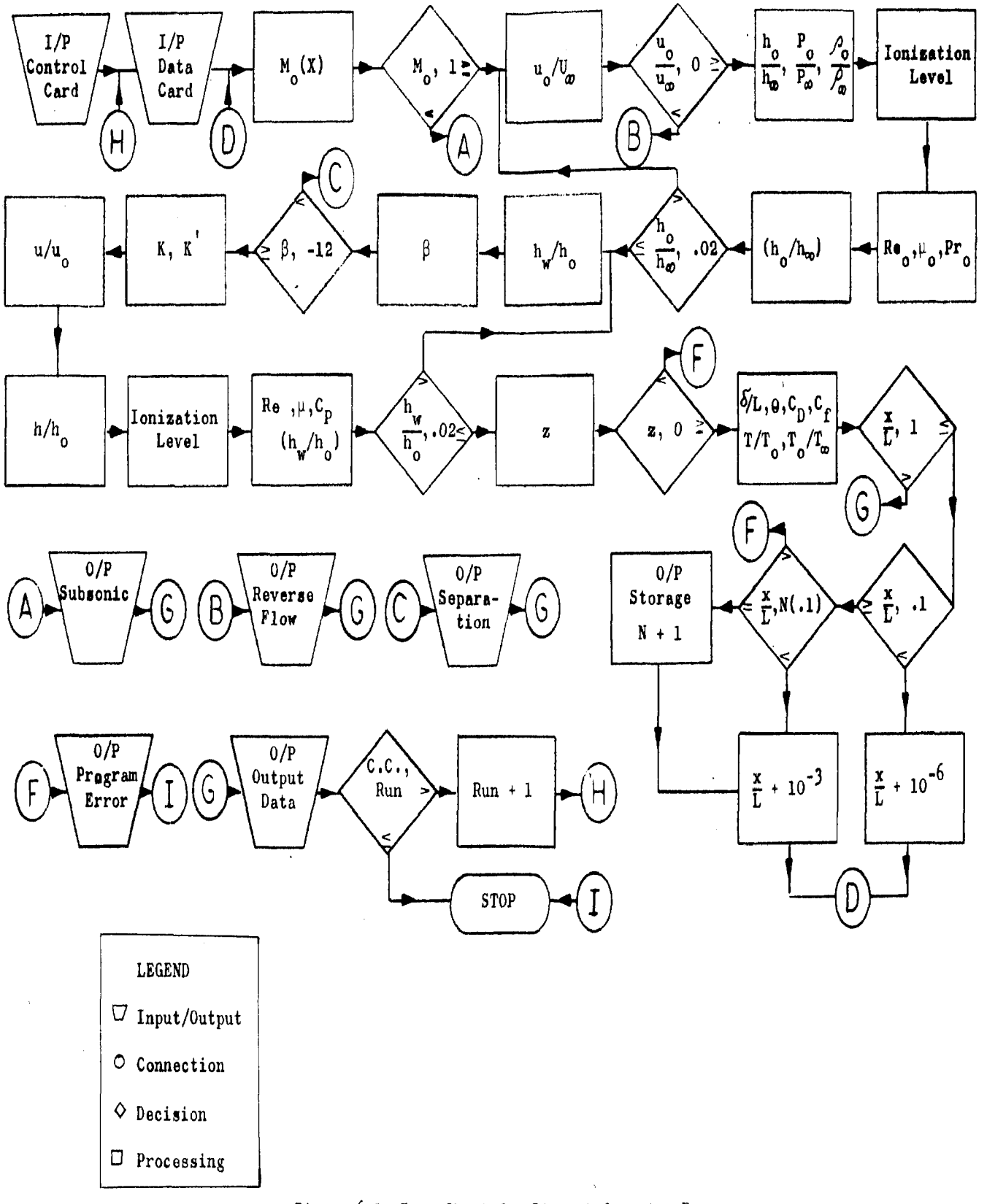

Figure 6.1 Flow Chart for Digital Computer Program

CHAPTER VII

CONCLUSIONS

Physical Limitations

A number of assumptions and simplifications have been made in order to obtain solutions to the problem presented in Chapter IV. It is the purpose of this section to investigate the physical limitations as they affect the range of application of the solutions.

In order to determine an approximate upper limit for the Hartmann number, Ha, the variables appearing in this dimensionless group will be considered separately. von Kármán (15) shows that the electrical conductivity of air is about 1.5 mhos/inch for a flow at Mach 20 and a density of 10^{-1} atmospheres, approximately an elevation of 59,000 feet. In the section on electrical conductivity it has been pointed out that the electrical conductivity does not vary greatly with density. Thus 1.5 mhos/inch will be considered as an upper limit for a physically realizable electrical conductivity for air.

The magnetic flux density which can be created in the boundary layer will depend on allowable coil size, power available, etc.; however, with a permanent magnet 1000 lines/inch^2 (155 Gauss) is not unreasonable.

A calculation for air viscosity versus temperature for air by Moore (19) shows that slightly ionized air has a coefficient of viscosity of roughly 10^{-6} slugs/ft-sec.

While the length of the plate is arbitrary, 60 inches is used.

In terms of the units given above

$$Ha^2 = \frac{\sigma B^2 L^2}{\mu} = \frac{1.8348 \times 10^{-11} (\sigma, \text{Mho/in}) (B, \text{lines/in}^2)^2 (L, \text{in})^2}{(\mu, \text{slugs/ft-sec})} \tag{7.1}$$

Substituting the arbitrary maximum values defined above

$$Ha \approx 125 \tag{7.2}$$

Since the solutions for the flat plate are based on the assumption of laminar flow in the boundary layer, the critical Reynolds number must be considered. When the air stream is very free from disturbances, values up to 3×10^6 have been found for the critical Reynolds number (reference 22). Thus 10^6 may be considered as a reasonable upper limit for the Reynolds number.

In developing the equations of motion, it has been assumed that the ionized gas is a continuous fluid in order to apply the macroscopic equations of fluids and electromagnetic theory to the problem. Tsien (26) suggests that the realm of continuum gas dynamics may be assumed if the order of $Re^{1/2}/M$ is about 100 or greater. Assuming a

maximum Reynolds number of 3×10^6 limits the Mach number to about 18.

Example Problem

In the limiting case of zero magnetic field, i.e., Ha = 0, the solution of the flow characteristics for an ionized gas over a flat plate has been found to reduce to the results presented by Schlichting (22) and von Kármán (14).

In order to present the effects of the various parameters involved in the problem the following values have been selected as typical for the free stream conditions:

M : 5, 15;

Re: 10^5, 10^6;

Pr: 0.721, 1;

Ha: 0, 10, 50, 100.

For the purposes of comparison, the following variables have been held constant:

$$\gamma = 1.4$$

$$\left(\frac{dP}{dx}\right)_{applied} = 0.$$

While solutions for all combinations of the above variables are not presented in the following pages, sufficient combinations are included to demonstrate the results. It should

be noted that because of the physical limitations presented earlier some combinations are not valid.

Figures 7.1 and 7.2 (plots begin on page 71) present typical solutions for the inviscid flow region. The Mach number and the velocity decay exponentially with distance along the plate while the temperature, density, and pressure increase. Figure 7.1 demonstrates the fact that for higher Mach numbers a greater influence is exerted by the same magnetic field because of the increase in electrical conductivity due to the increase in temperature. Particular notice should be made of the adverse pressure gradient shown in Figure 7.2. Further comment on this will be made in connection with body shape factor and separation.

Figures 7.3 and 7.4 show the effects of the magnetic field on the boundary layer thickness for M_∞ of 5 and 15 for constant Reynolds and Prandtl numbers. The variation of the boundary layer thickness with the Reynolds number is similar to that of ordinary flow, i.e., $\delta \propto 1/\sqrt{Re}$. The boundary layer thickness increases with the Hartmann number, as might be expected by the adverse pressure gradient, causing the velocity gradient at the plate surface to decrease and thus decreasing the skin friction coefficient as shown in Figure 7.5. This is consistent with the effect Rossow (20) predicted for the case of no pressure gradient and incompressible flow and is consistent with ordinary flow as presented by Schlichting (22, Chapter XV).

The overall drag coefficient has been defined in terms of the wake drag. Since the upper limit of the integral appearing in equation 6.73 has been taken as the Mach line it is necessary to insure that the boundary layer thickness is less than or equal to $L\tan\mu$ at $x = L$. The computer program incorporates a check routine to insure this condition is met. The contribution due to the magnetic influence in Region 2 is approximately two percent of the contribution from the boundary layer, Region 3, for each additional increment of δ. In the cases considered the upper limit was approximately three times the value of δ. Figure 7.6 shows the variation of the overall drag coefficient.

A sample velocity profile is presented in Figure 7.7. It has been found that the velocity reaches the inviscid value more slowly as the effect of the magnetic field is increased. For the case of a particular field strength, the electrical conductivity increases with distance along the plate resulting in an increase in the local magnetic influence parameter; hence, a shift in the velocity profile occurs. It should be noted that u_e also varies with distance along the plate (Figure 7.2).

A sample temperature profile is presented in Figure 7.8. As a result of internal heat generation, the temperature in the magnetic case is greater than that in the ordinary case. No consideration has been given to the

fact that the thermal boundary layer thickness and the momentum boundary layer thickness are different. As was pointed out in Chapter IV, the thermal boundary layer thickness can be much larger than the velocity boundary layer thickness when the Prandtl number is not approximately unity.

The body shape factor, β, is a measure of the pressure gradient along the plate. Equation 6.9 shows that separation occurs for $\beta = -12$. Figure 7.9 shows the variation of β with distance along the plate for various Hartmann numbers and $M_\infty = 15$. Since it has been assumed that the applied pressure gradient is zero, for a zero Hartmann number $\beta = 0$. As the Hartmann number increases, β increases negatively, and for sufficiently high values of the Hartmann number separation occurs.

Approximate Solutions

Two useful equations can be obtained from the computer solutions by fitting curves to the data. The boundary layer growth may be expressed as

$$\frac{\delta}{L} = 2.12\left(1 + \frac{\gamma-1}{2}M_\infty^2\right)^{.701} (Re)_\infty^{-.501} \left(\frac{x}{L}\right)^{.750} e^{Ha_\infty(8.6M_\infty + 11.0)10^{-4}} \tag{7.3}$$

while the location of separation may be expressed as

$$Re_x = \frac{\rho_\infty u_\infty x}{\mu_\infty} = 4.03 \times 10^9 (M_\infty)^{-1.51} (Ha_\infty)^{-1.113} \tag{7.4}$$

The error resulting from these equations is less than 5% in the ranges:

$$.1 \leq x/L \leq 1;$$

$$5 \leq M_\infty \leq 20;$$

$$0 \leq Ha_\infty \leq 10^3;$$

$$10^4 \leq Re_\infty \leq 3 \times 10^6.$$

Equation 7.3 is not valid once separation occurs. Equation 7.3 overestimates the thickness near the leading edge by a factor of 10 or more. Equation 7.4 predicts separation earlier than the computer solution for the low Mach numbers. Figures 7.10 and 7.11 show the approximate solutions and the computer solutions for the boundary layer thickness and the location of the separation point respectively.

Summary

The results of this analysis show that a significant change in the boundary layer thickness and the total drag is possible for reasonable values of electrical conductivity and magnetic field strength. Also it has been demonstrated that separation can be induced by the application of a magnetic field. It should be recalled that this effect is due to the induced pressure gradient. For large Mach numbers, all results are more sensitive to variations in the Hartmann number. Since the magnetic effect is velocity dependent, the increased effect is reasonable. Finally, it has been established that the velocity and the

temperature vary with position along the plate. Hence a true similarity condition does not exist as in the case of ordinary flow (Blasius solution). In all cases, the solutions reduce to within one percent of those given in Schlichting (22) and von Kármán (14) for ordinary flow. While no experimental results are available at the present, the assumptions made indicate results which, when compared with experimental results, should be within the error limits of current ordinary boundary layer analysis.

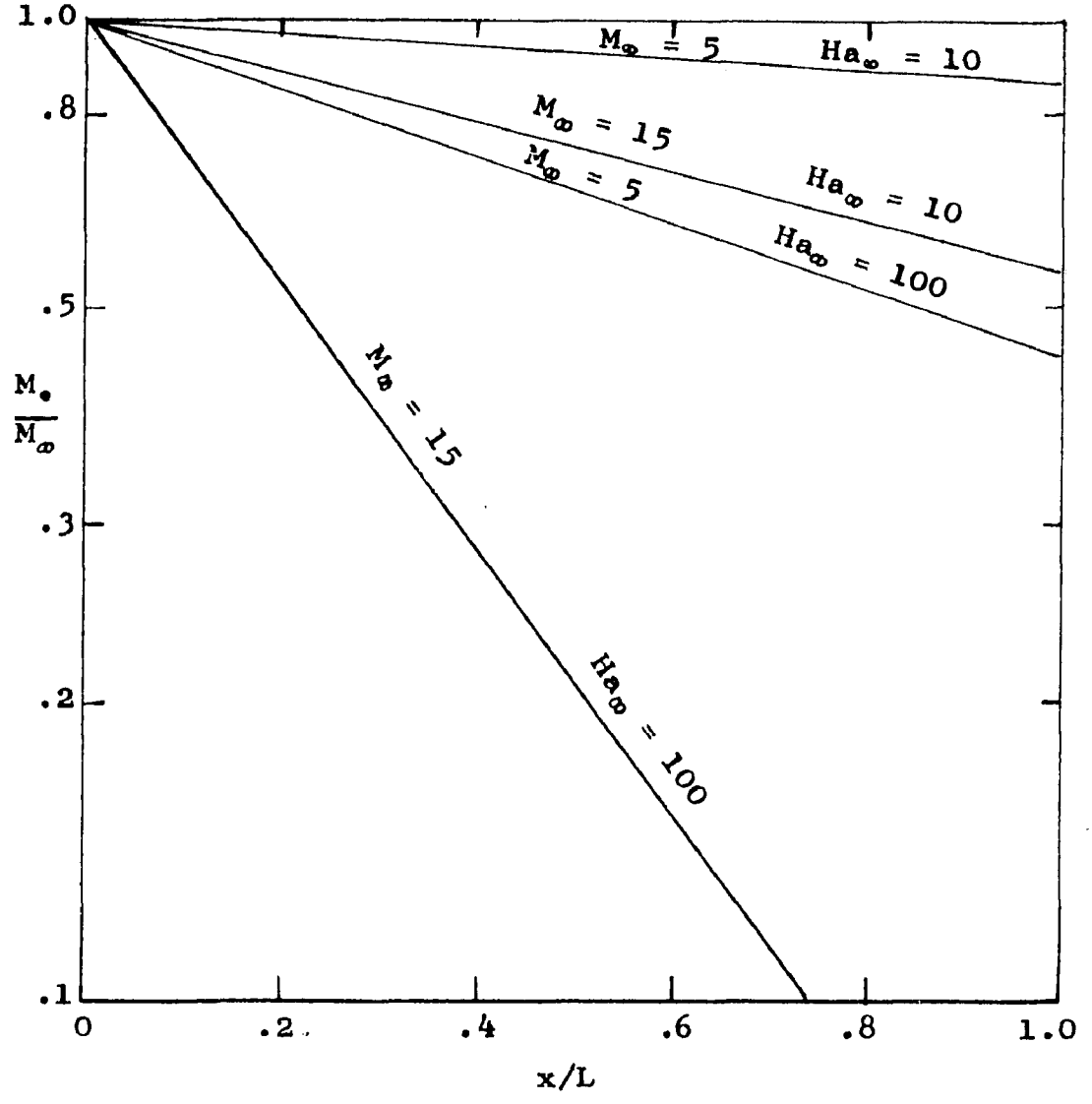

Figure 7.1 Mach Number Decay in Region 2

$Re_\infty = 10^6$, $Pr_\infty = 0.721$

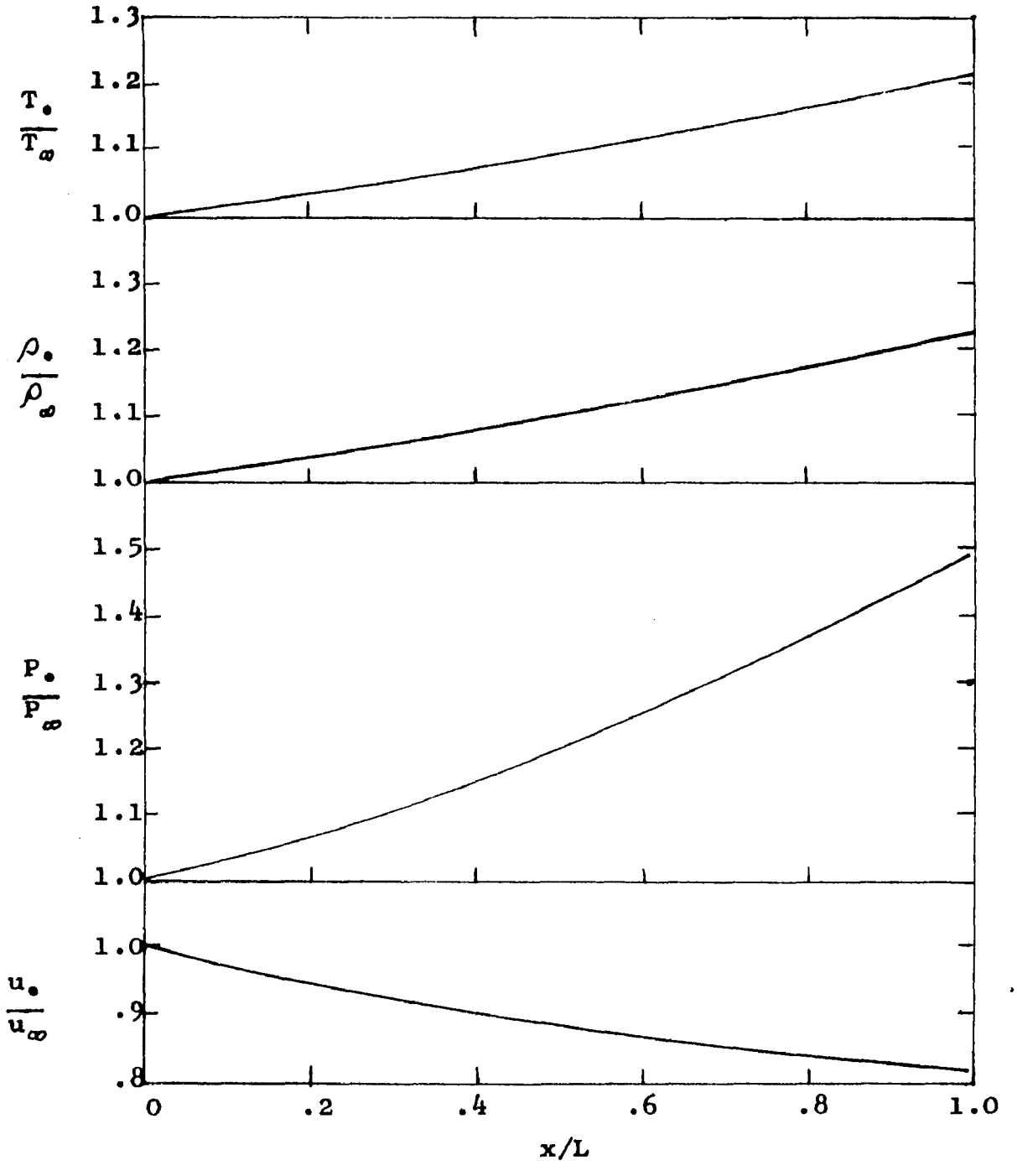

Figure 7.2 Flow Parameters in the Inviscid Region

$M_\infty = 15$, $Pr_\infty = 0.721$

$Re_\infty = 10^6$, $Ha_\infty = 10$

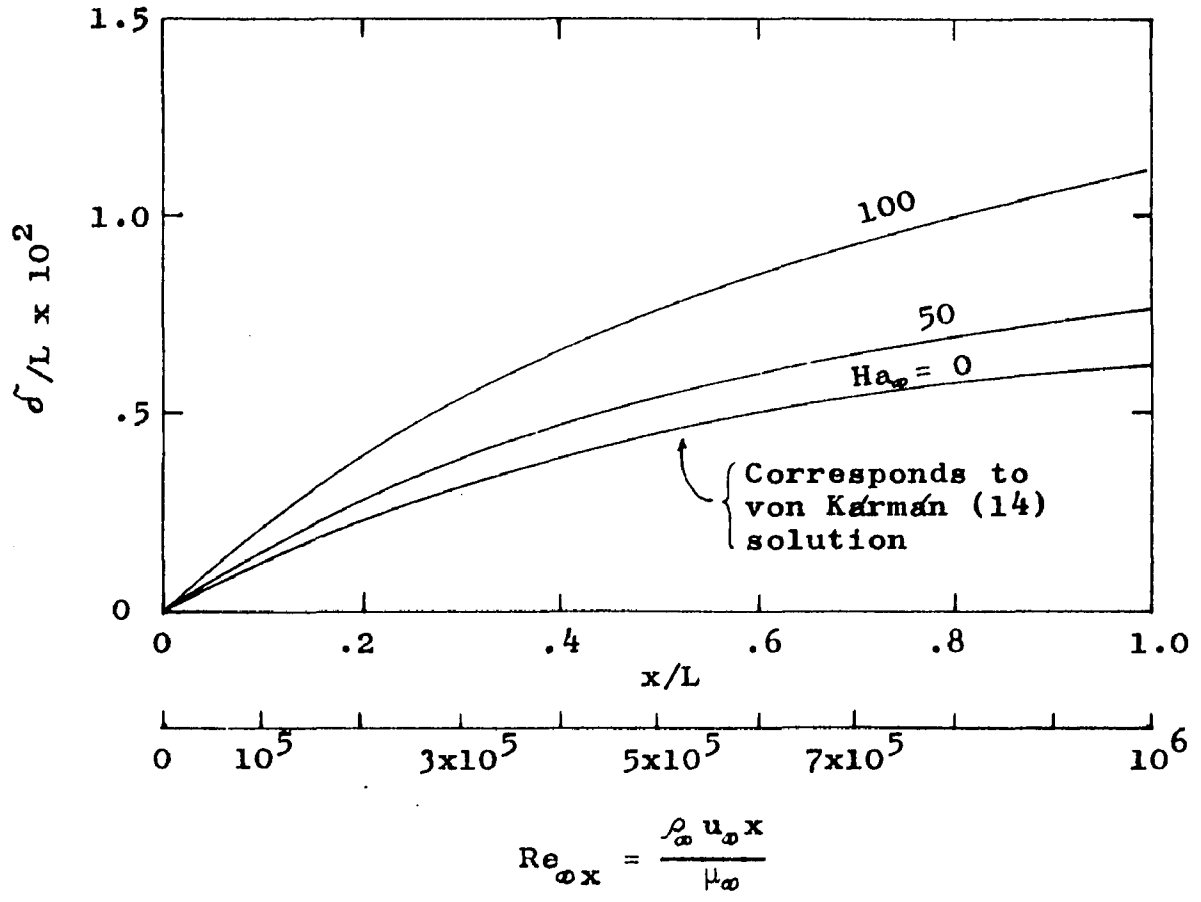

Figure 7.3 Boundary Layer Development

$M_\infty = 5$, $Re_\infty = 10^6$

$Pr_\infty = 0.721$, L = 60 inches

The profile for Ha = 0 is within 1% of that given by von Kármán for laminar compressible flow (14).

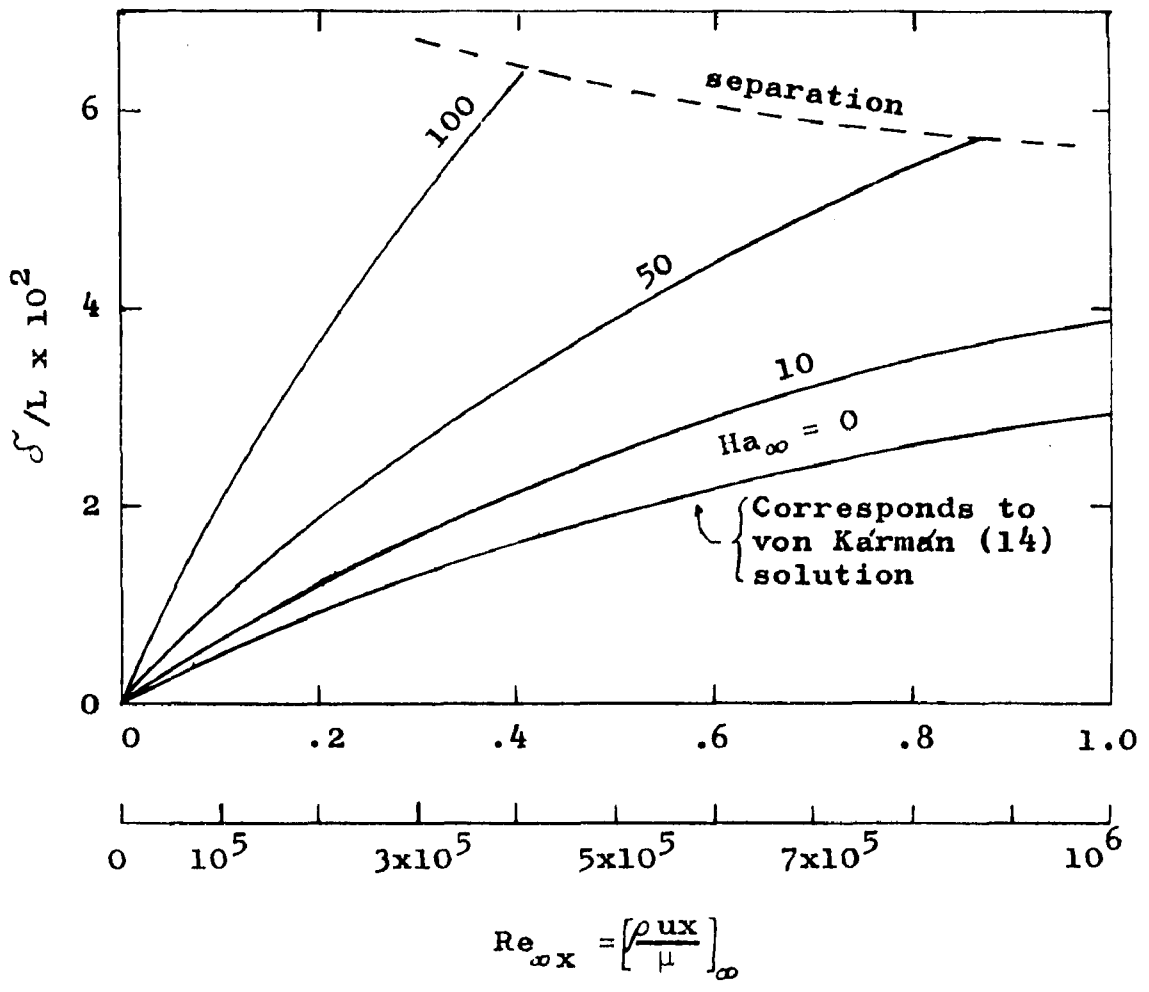

Figure 7.4 Boundary Layer Development

$M_\infty = 15$ $\quad Re_\infty = 10^6$

$Pr_\infty = 0.721$ $\quad L = 60$ inches

The profile for $Ha_\infty = 0$ is within 1% of that given by von Kármán for laminar compressible flow (14).

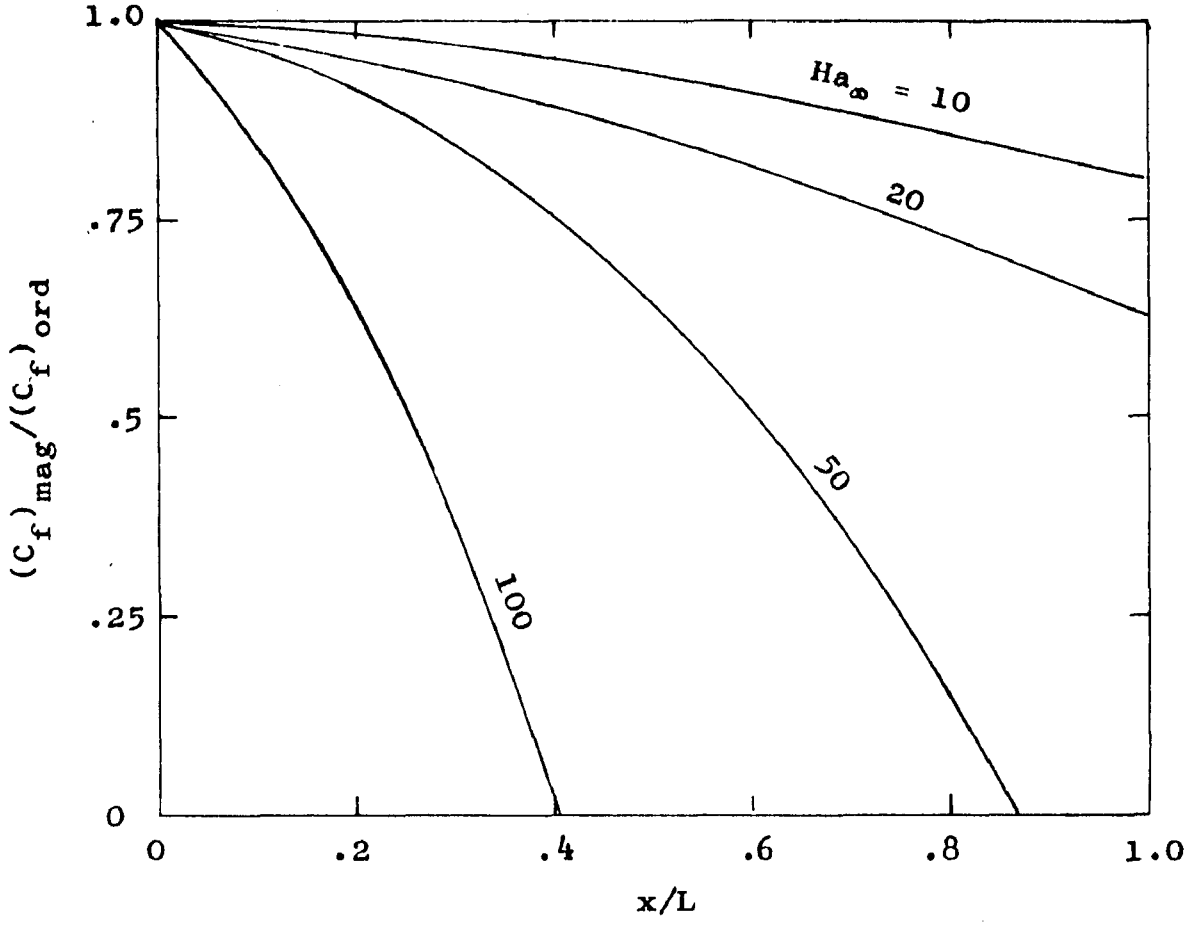

Figure 7.5 Local Skin Friction Coefficient Variation Along the Plate

M_∞ = 15 $Re_\infty = 10^6$

Pr_∞ = 0.721

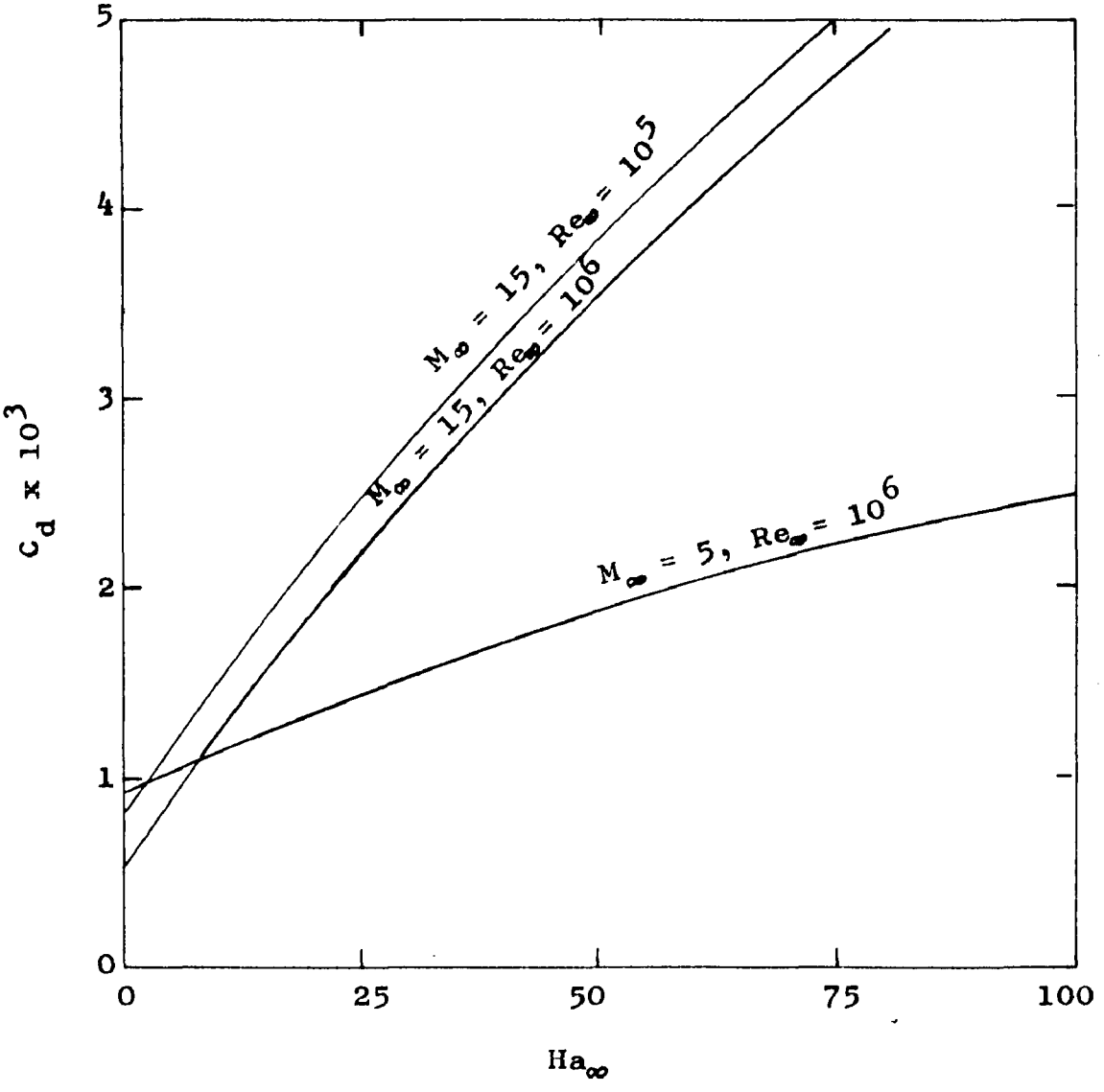

Figure 7.6 Coefficient of Total Drag for Laminar Flow Region

$Pr_\infty = 0.721$

L = 60 inches

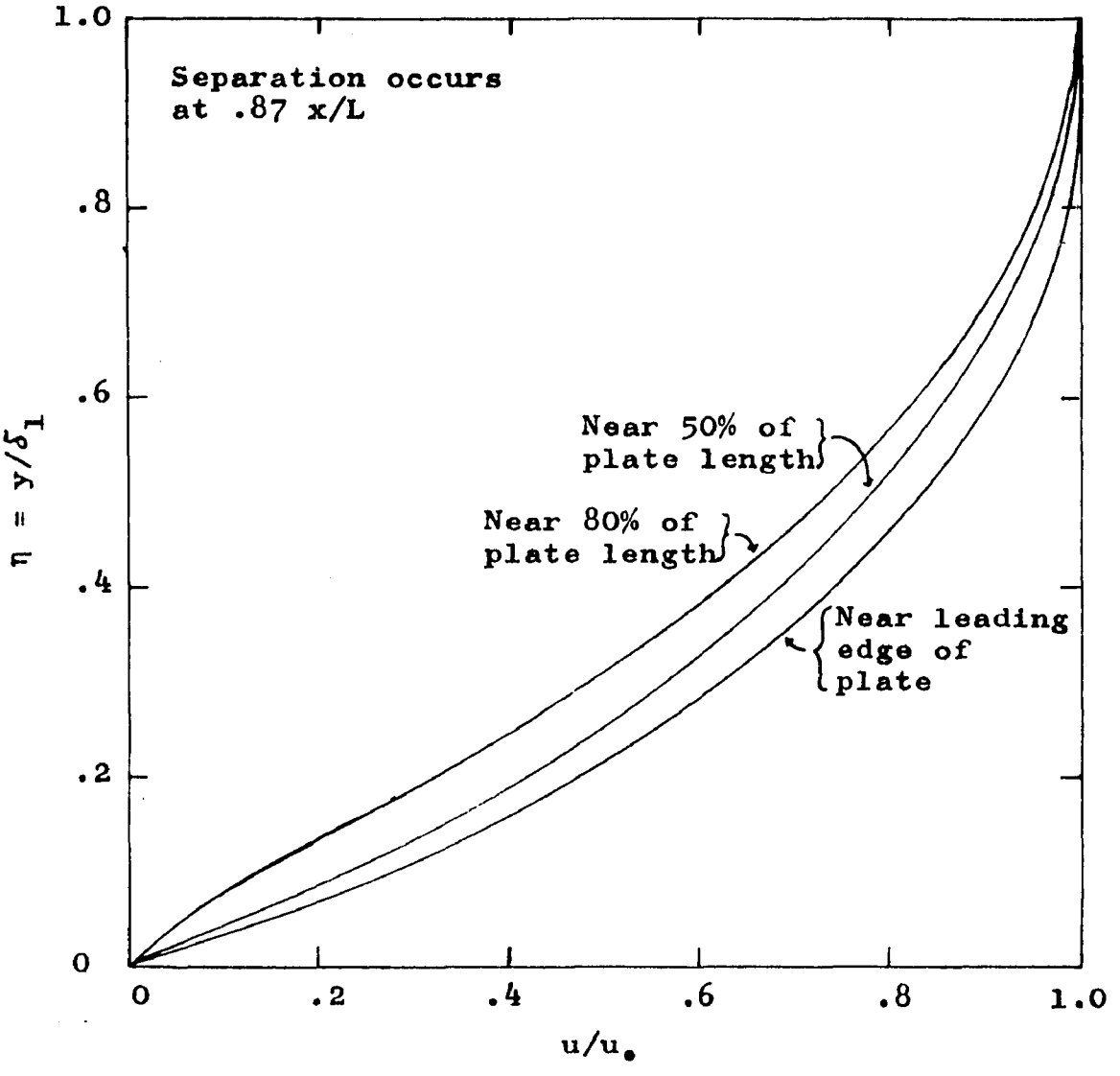

Figure 7.7 Boundary Layer Velocity Profile

$M_\infty = 15$, $Re_\infty = 10^6$

$Ha_\infty = 50$, $Pr_\infty = 0.721$

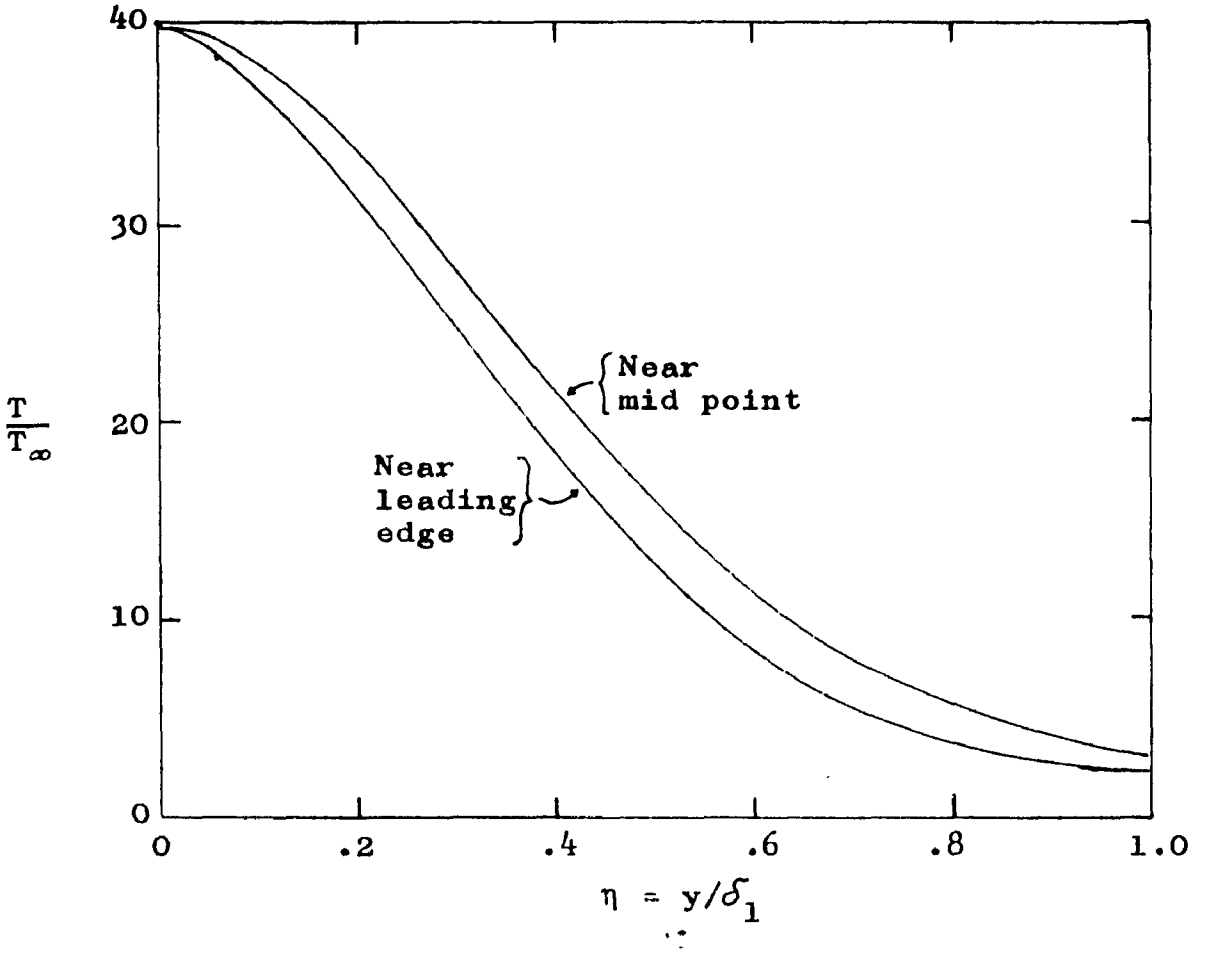

Figure 7.8 Boundary Layer Temperature Profile

$M_\infty = 15$, $Re_\infty = 10^6$

$Pr_\infty = 0.721$, $Ha_\infty = 50$

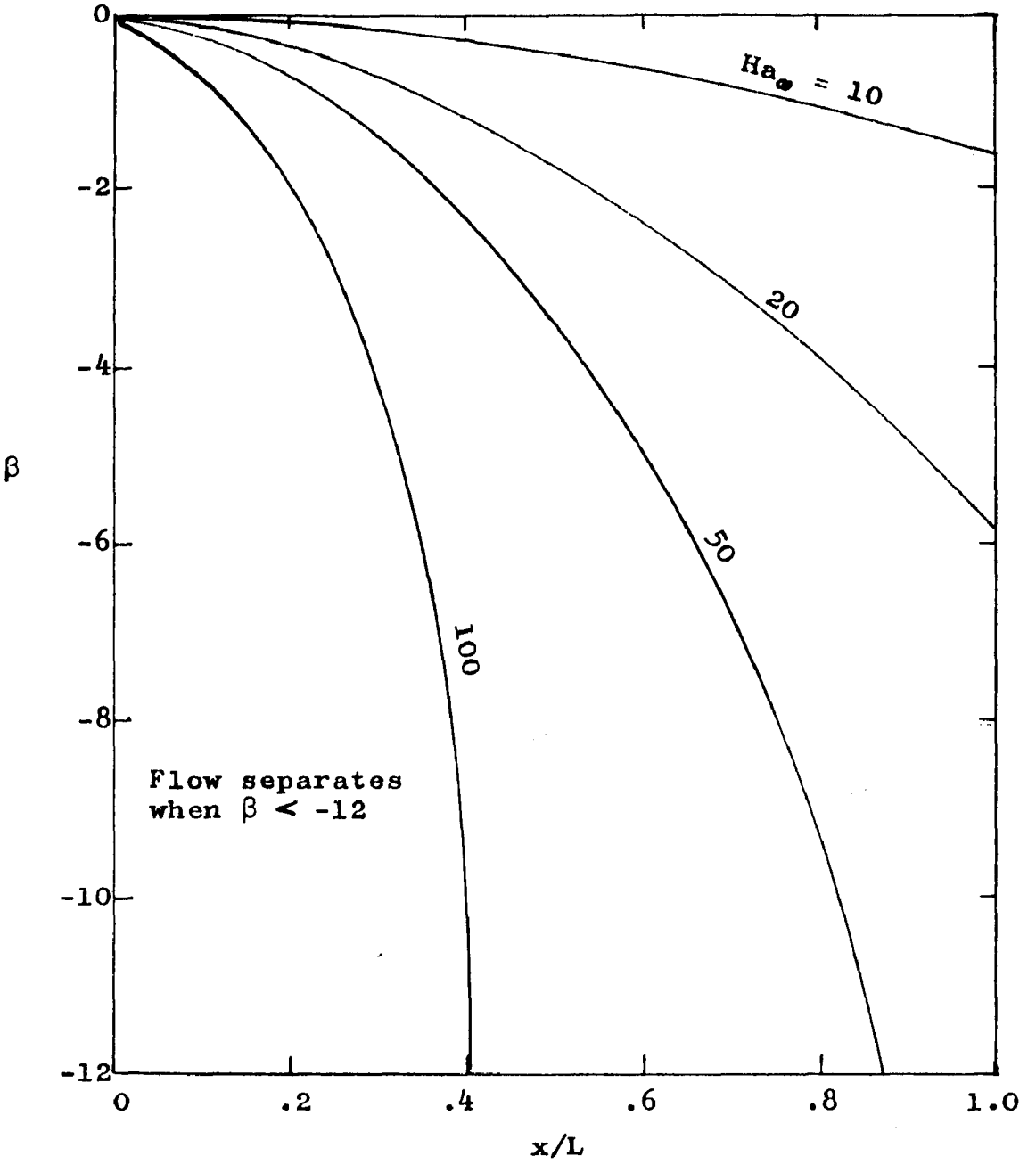

Figure 7.9 Body Shape Factor

$M_\infty = 15, \qquad Re_\infty = 10^6$

$Pr_\infty = 0.721$

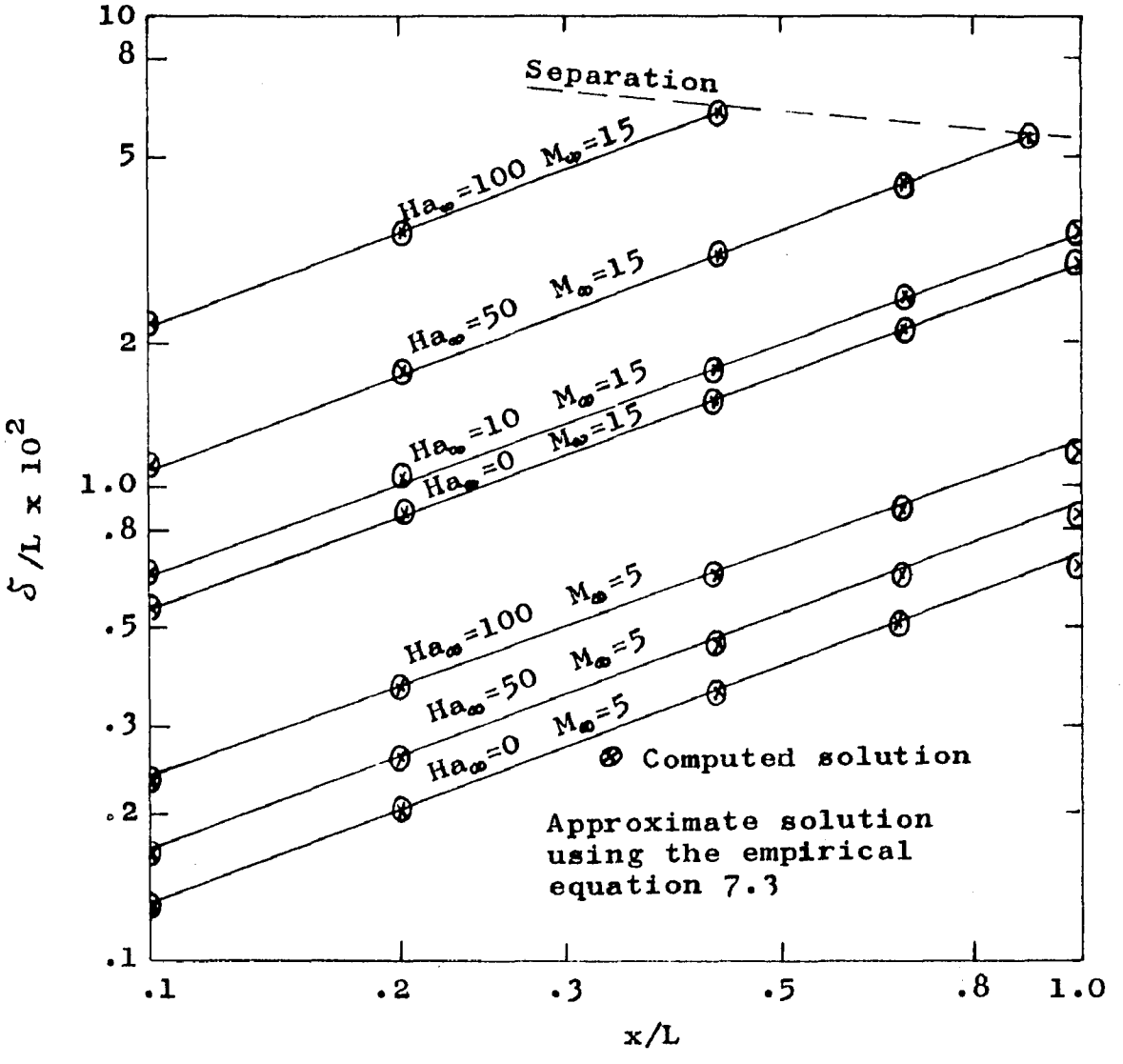

Figure 7.10 Approximate Boundary Layer Development

$L = 60$ inches, $\quad Re_\infty = 10^6$

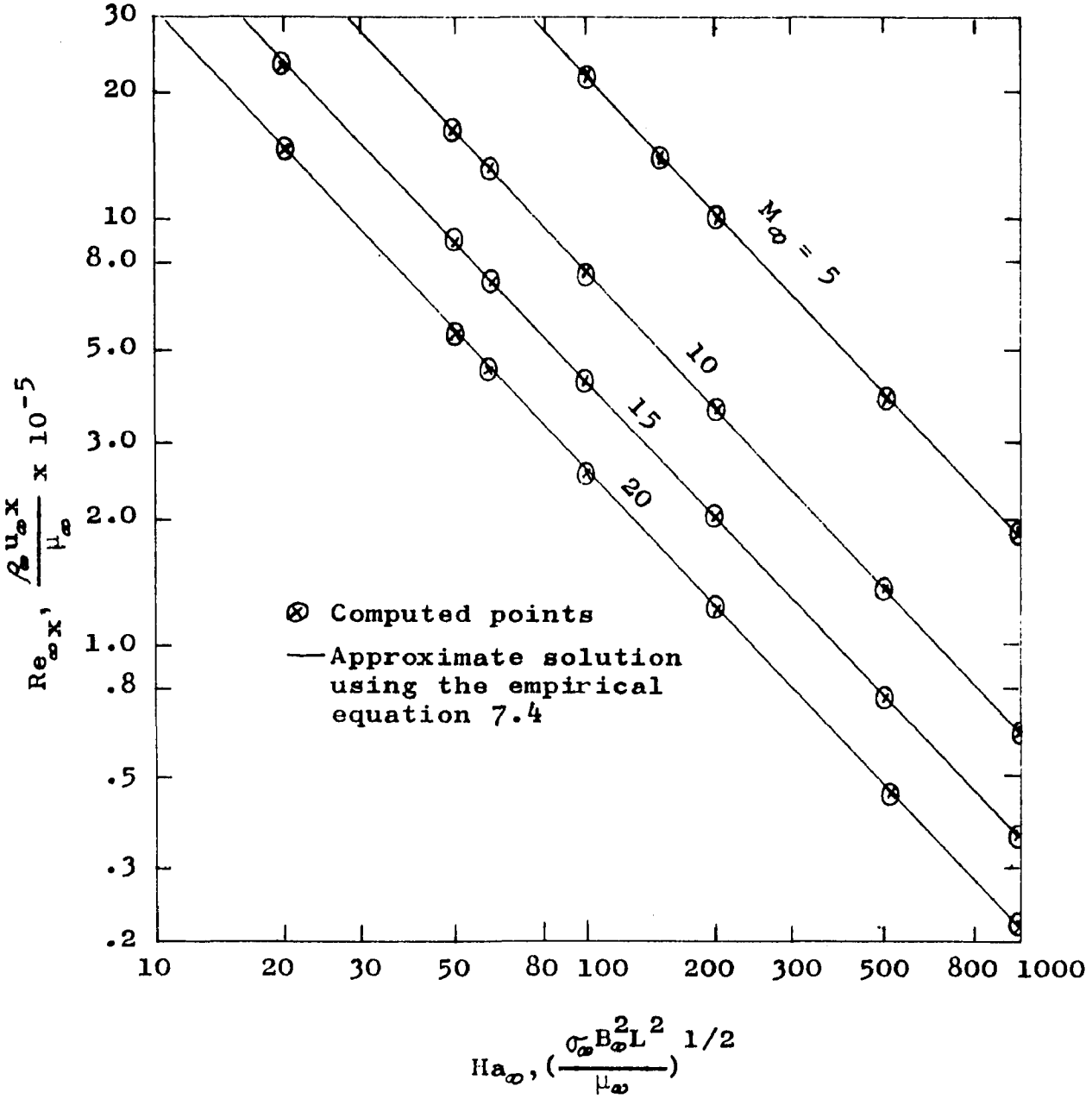

Figure 7.11 Location of Separation Point

$\beta = -12$, L = 60 inches

APPENDICES

APPENDIX A

ENERGY EQUATION ANALYSIS

It has been demonstrated in Chapter VI that for the case of an adiabatic wall the enthalpy ratio may be expressed as a function of u. If, in a more general case, we assume the enthalpy can be expressed as

$$h = a + bu + cu^2 \tag{A.1}$$

the energy equation, with Pr = 1, may be written as

$$(b+2cu)(\rho uu_y+\rho vu_y)+\rho(u^2b_x+c_xu^3+a_xu)$$

$$= u\frac{dP_e}{dx} + \sigma B_\infty^2u^2+\mu u_y^2+\mu 2c(u_y^2+uu_{yy})+\mu bu_{yy}+\mu(b_xu+c_xu^2) \tag{A.2}$$

Multiplying the momentum equation by b +2cu and subtracting the resulting expression from equation A.2 yields

$$\rho u(a_x+b_xu+c_xu^2) = b(\frac{dP_e}{dx} + \sigma B_\infty^2u)$$

$$+ (2c+1)u(\frac{dP}{dx} + \sigma B_\infty^2u)$$

$$+ \mu u(b_x+c_xu)$$

$$+ \mu(2c+1)u_y^2 \tag{A.3}$$

Since equation A.3 must hold at the wall

$$0 = b\frac{dP_e}{dx} + \mu_w(2c+1)(u_y^2)_w \tag{A.4}$$

If $b \neq 0$, c must be at least a function of x and the wall shear. Returning to equation A.3 and equating like powers of u, the coefficient of u^3 is

$$c_x = 0 \qquad (A.5)$$

which contradicts equation A.4. Also, since the velocity gradient varies through the boundary layer, it is not possible to eliminate the non-linear term appearing in equation A.3.

If the coefficient of u^2 is considered, it is found that

$$b_x = f(u, u_y, c, c_x) \qquad (A.6)$$

which is contrary to the assumption that b and its derivatives are not functions of u. Hence it must be concluded that equation A.1 is wrong unless $b = 0$, which is the adiabatic wall condition.

If a, b, and c are considered as functions of x and y, the same contradictions result. This is to be expected since u is primarily a function of y.

If the velocity gradient is assumed to be a constant (a fair approximation for hypersonic flow), it is possible to obtain the following differential equation for the enthalpy ratio, $h^* = h/h_\bullet$,

$$h^{*''}+PrRe\frac{dz}{dx}(1+\eta)h^{*'}+PrRe\frac{(\gamma-1)}{2}M_\infty^2 z h^*$$

$$= -Pr(\gamma-1)M_\infty^2-RePr\frac{(\gamma-1)}{2}M_\infty^2 z\frac{1}{\rho_\infty u_\infty^2}\frac{dP}{dx^*} \qquad (A.7)$$

This equation may be used to replace equations 6.79 and 6.82 in the computer program. It should be noted that P(x), equation 6.50, is also changed. The resulting program exceeds 10,000 words which is the word storage on the available system.

Since the resulting equations for z and h* are coupled by their derivatives, the following process could be used to obtain a computer solution.

1. $z_{adiabatic}$ is calculated for a given x.
2. h* and its derivatives are calculated based on the adiabatic solution.
3. z is again calculated, as is h* based on equation 6.29.
4. A variation in either variable greater than an acceptable error causes a recycling, otherwise a new value of x is calculated.

For one set of free stream flow conditions, this analysis required approximately two hours of computer time to reach a quarter of the length of the plate ($\Delta x = 0.25$). It is estimated that approximately one hundred hours of computer time would be necessary to obtain sufficient information

for valid conclusions. Therefore, the run was discontinued due to the small amount of additional relevent information which could be obtained.

APPENDIX B

FORTRAN LANGUAGE PROGRAM

The following Fortran Language program was used to obtain the solution of the set of equations for the adiabatic flat plate. As it is presented here, each equation number denotes one Fortran statement as it would appear when the standard card format is used. In a few cases the statement length exceeds the field length permitted for cards. In practice, such statements are placed on two or more cards. However, for the purpose of clarity, the statement is written as if it could be placed on one card. Data cards would follow the program in the case of an actual computer run. All data cards use a floating point format. The first data card is the number of sets of free stream data. The number begins in column 7. The following card or cards are the free stream conditions for a particular problem. Each card has the following format: the Mach number, beginning in column 11; the Hartmann number, beginning in column 21; the Reynolds number, beginning in column 31; the ratio of specific heats, beginning in column 41; the Prandtl number, beginning in column 51; and the length of the plate in inches, beginning in column 61. The time required to complete the analysis

for one set of free stream conditions is approximately five minutes exclusive of the time required for compiling and printing.

```
    1 FORMAT (10X, 6F10.0)                                          (B.1)

    2 FORMAT(30H   FLOW GOES SUBSONIC AT X =  1PE20.8)              (B.2)

    4 FORMAT (1HO 16X,1HX 18X,4HBETA 13X,10HLOCAL
      MACH  13X,5HDELTA)                                            (B.3)

    5 FORMAT (1HO 3X,1P4E20.7)                                      (B.4)

    6 FORMAT (1H1  8H  MI = (1PE13.4), 8H  MPI =
      (1PE13.4))                                                    (B.5)

    7 FORMAT (9H   TI =    1PE13.4),  8H  RE =
      (1PE13.4))                                                    (B.6)

    8 FORMAT (1HO 16X, 1HX 17X, 5HTHETA 14X,11HDRAG
      COEFF. 8X, 10HSKIN FRICT )                                    (B.7)

    9 FORMAT (1HO 3X, 1P4E20.7)                                     (B.8)

   19 FORMAT (3X, 1P4E20.7)                                         (B.9)

   26 FORMAT (6X, 1F8.0)                                            (B.10)

   60 FORMAT (9X, 8HFOR X = 1PE20.7, 11X, 8HFOR X =
      1PE20.7)                                                      (B.11)

   61 FORMAT (10X, 3HETA 187, 4HU/U0 22X,3HETA 19X,
      4HU/U0)                                                       (B.12)

   62 FORMAT (3X, 1P2E20.7, 5X, 1P2E20.7)                           (B.13)

  127 FORMAT(16X,1HX16X,6HU0/U0016X,6HT0/T0016X,
      6HP0/P0016X,6HD0/D00)                                         (B.14)

  128 FORMAT (1HO 3X, 1P5E20.7)                                     (B.15)

  140 FORMAT (1HO)                                                  (B.16)

  209 FORMAT (32H  INCORRECT DATA FORMAT CARD   )                   (B.17)

  215 FORMAT (38H  ORDER OF PRINT OUT AB1,AB,XL1,
      XL,EB  )                                                      (B.18)
```

```
  216 FORMAT (3X, 1P5E20.7)                                          (B.19)
  521 FORMAT (4X, 3HETA 17X, 1HH 19X, 1HH 19X,
      1HH 19X, 1HH  )                                                (B.20)
  522 FORMAT (3X, F6.3, 1P4E20.7)                                    (B.21)
  523 FORMAT (3X, 9HFOR X =  4E20.7)                                 (B.22)
      DIMENSION UOI(105), TOI(105), PII(105),
      ROI(105)                                                       (B.23)
      DIMENSION BEI(105),DELI(105),FMAJ(105),XI(105)                 (B.24)
      DIMENSION THEI(105), CFI(105)                                  (B.25)
      DIMENSION DUDI(105), UUI(105,11),  ETI(11)                     (B.26)
      DIMENSION FOC2(4), FLC(4), TC(4), Q1(4), P1(4)                 (B.27)
      DIMENSION A4(4), FHI(105,11)                                   (B.28)
      QI = 4.8                                                       (B.29)
      BK = 0.1380                                                    (B.30)
      TINF = 530.                                                    (B.31)
      DX = 0.001                                                     (B.32)
      E = 2.718282                                                   (B.33)
      AK = 0.0                                                       (B.34)
      READ 26, AJ                                                    (B.35)
   30 READ 1, FMAI, FHA, RE, G, FLE, PR                             (B.36)
      FL = FHA*FHA/RE                                                (B.37)
      FMI = 12.*FL/FLE                                               (B.38)
      PR = PR/2.                                                     (B.39)
C     INVISCID MACH NO. DECAY THRU STM 207                           (B.40)
      IF (FL) 208,206,205                                            (B.41)
  208 PRINT 6,FMAI,FL                                                (B.42)
      PRINT 7, TINF, RE                                              (B.43)
```

```
      PRINT 209                                                    (B.44)
      GO TO 403                                                    (B.45)
206   EB = 0.0                                                     (B.46)
      GO TO 207                                                    (B.47)
205   AB1 = (1. +(G-1.)*FMAI*FMAI/2.)/(1.+G-1)*0.32*
      FMAI*FMAI)                                                   (B.48)
      AB = 0.64*(AB1**((G+1.)/(G-1.)))                             (B.49)
      XL1 = LOGEF(AB)                                              (B.50)
      XL = XL1/(2.0*G*FL*FMAI*FMAI)                                (B.51)
      EB = -XL1/(FL*XL)                                            (B.52)
      IF(EB) 207,212,212                                           (B.53)
212   PRINT 6, FMAI, FL                                            (B.54)
      PRINT 7, TINF, RE                                            (B.55)
      PRINT 215                                                    (B.56)
      PRINT 216, AB1,AB,XL1,XL,EB                                  (B.57)
      GO TO 403                                                    (B.58)
207   AK = AK +1.0                                                 (B.59)
 64   DUDY = 1.0                                                   (B.60)
      UO = 1.0                                                     (B.61)
      TO = 1.0                                                     (B.62)
      PI = 1.0                                                     (B.63)
      RO = 1.0                                                     (B.64)
 65   UUO = 1.0                                                    (B.65)
      X = 0.0                                                      (B.66)
      THE = 0.0                                                    (B.67)
      CFX = 0.0                                                    (B.68)
```

```
      BE = 0.0                                                    (B.69)
      DEL = 0.0                                                   (B.70)
10    GH = (G-1.0)/2.                                             (B.71)
      FMI2 = FMAI*FMAI                                            (B.72)
      GM = GH*FMI2                                                (B.73)
      ST = SQRTF(TI)                                              (B.74)
      FO = 1./FMAI                                                (B.75)
      FMU = FO +(FO**3)/6. +3.*(FO**5)/40. +5.*
     (FO**7)/128.                                                 (B.76)
      Z1 = 0.0                                                    (B.77)
      II = 1                                                      (B.78)
      I = 1                                                       (B.79)
      DO 300 J = 1,1001                                           (B.80)
      FMAO = FMAI*E**(EB*FL*X)                                    (B.81)
      IF(FMAO-1.)11,11,12                                         (B.82)
11    GO TO 399                                                   (B.83)
12    IF(II-J) 13,14,15                                           (B.84)
13    GO TO 403                                                   (B.85)
14    FMAJ(I) = FMAO                                              (B.86)
      UOI(I) = UO                                                 (B.87)
      TOI(I) = TO                                                 (B.88)
      PII(I) = PI                                                 (B.89)
      ROI(I) = RO                                                 (B.90)
      BEI(I) = BE                                                 (B.91)
      DELI(I) = DEL *FLE                                          (B.92)
      XI(I) = X                                                   (B.93)
```

```
   67 DUDI(I) = DUDY                                          (B.94)
      THEI(I) = THE*FLE                                       (B.95)
      CFI(I) = CFX                                            (B.96)
C     VELOCITY PROFILE                                        (B.97)
   92 ET = 0.0                                                (B.98)
   93 DO 100 L = 1,11                                         (B.99)
   95 FBE = 2.0*ET -2.0*(ET**3) +ET**4                        (B.100)
   96 GBE = (ET -3.0*(ET**2) +3.0*(ET**3)
      -ET**4)/6.0                                             (B.101)
   97 UUI(I,L) = FBE + BE*GBE                                 (B.102)
      ETI(L) = ET                                             (B.103)
   98 ET = ET + 0.1                                           (B.104)
  100 CONTINUE                                                (B.105)
C     INVISCID FLOW THRU 71 +2                                (B.106)
   15 FMA0 = FMAI*E**(EB*FL*X)                                (B.107)
      FMA2 = FMA0*FMA0                                        (B.108)
      FM = FMI* FMI2/FMA2                                     (B.109)
      GM0 = FMA2*GH                                           (B.110)
   68 E1 = E**(2.0*EB*FL*X)                                   (B.111)
      EB1 = G*FMI2/(2.*EB)                                    (B.112)
      E2 = E**(G*(G-1.)*FMI2*FL*X)                            (B.113)
      U02 = (FMI2 -1.)/(FMI2*E1 -1.)                          (B.114)
      U01 = U02**EB1                                          (B.115)
      U0 = E2*U01                                             (B.116)
      IF(U0)399,70,71                                         (B.117)
   71 T0 = E2/(U0**(G-1.0))                                   (B.118)
```

```
      PI = TO/UO                                                    (B.119)
      RO = 1.0/UO                                                   (B.120)
C     DELTA ITERATION THROUGH STMT 99                               (B.121)
   70 FK = -G*FL*FMI2/(FMA2-1.0) + FL*FMI2/FMA2                     (B.122)
      FKP = -G*FL*GMI2/(FMA2-1.)                                    (B.123)
   43 AA = 37./315. -BE/945. -BE*BE/9072.                           (B.124)
      B = 8113./4045. -97.*BE/90090.0 -379.*BE*BE
     /2162160.0 -BE*BE*BE/617760.                                   (B.125)
      Q = (12.+BE)*(12.+BE)/2160.0                                  (B.126)
      G1 = (2. -(B -PR*Q)/AA)*GH                                    (B.127)
      G2 = (2. -(B-Q)/AA)*GH                                        (B.128)
      G4 = (1.3 +19.*BE/120. -19.*(2. +BE/6.)
     /20.)*AA                                                       (B.129)
      T = TO*(FM*G4+(1. +FMA2*G1)/(1. +FMA2*G2))                    (B.130)
C     IONIZATION PERCENT                                            (B.131)
      XA = 0.001*SQRTF(E**(-QI/(BK*TINF))*TINF
     **1.25                                                         (B.132)
      XB = (E**(QI*(1.-TO)/(BK*TINF))*(TO**2.5)                     (B.133)
      FI = SQRTF(XB/(XA*XA*PI +XB)) *0.001                          (B.134)
      FMO = TO*(1.-FI) +TO**(5./2.)*FI                              (B.135)
  222 REI= RE*UO*RO/FMO                                             (B.136)
      PRI= PR*FMO/2.                                                (B.137)
      IF(ABSF(REI-RE) -0.02)220,220,221                             (B.138)
  221 RE = REI                                                      (B.139)
      PR = PRI                                                      (B.140)
      GO TO 70                                                      (B.141)
  220 CONTINUE                                                      (B.142)
```

```
      F1 = 1.0 +BE/12.                                          (B.143)
      F2 = 215.*BE*BE/9072. -871.*BE/7560. -33./70.             (B.144)
      F3 = -AA                                                  (B.145)
      F4 = 83./630. -79.*BE/7560. -BE*BE/4536.                  (B.146)
      F5 = 1. +BE/120.                                          (B.147)
   69 RAT = UO*F1*T/2.0                                         (B.148)
   16 CHI = X                                                   (B.149)
      DO 17 N = 1,3                                             (B.150)
      FOC = FMAI*E**(EB*FL*CHI)                                 (B.151)
      FOC2(N) = FOC*FOC                                         (B.152)
      FLC(N) = FL*FMI2/FOC2(N)                                  (B.153)
      TC(N) = TO*(FMI*FMI2*G4/FOC2(N) +(1. +FOC2
     (N)*G1)/(1. +FOC2(N)*G2))                                  (B.154)
   17 CHI = CHI + DX/2.                                         (B.155)
      DO 18 NN = 1,3                                            (B.156)
      Q1(NN) = F1/(AA*RE)                                       (B.157)
      PO = ((0.7+BE/120.)/(2.*AA) -(2.-FOC2(NN))
     /2.)*FKP                                                   (B.158)
      PP = (FL*FMI2*(.6-19,*TC(NN)*TC(NN)/20.)
     /FOC2(NN)-FK*(.6+.4*TC(NN)))/(2.*AA)                       (B.159)
   18 P1(NN) = PO +PP                                           (B.160)
      A1 = DX*(Q1(1)+P1(1)*Z1)                                  (B.161)
      A2 = DX*(Q1(2)+P1(2)*(Z1+A1/2.))                          (B.162)
      A3 = DX*(Q1(3)+P1(3)*(Z1+2.*A2 -A1))                      (B.163)
      Z2 = Z1 + (A1 + 4.*A2 + A3)/6                             (B.164)
      IF(Z2)20,21,21                                            (B.165)
   20 DI = ABSF(Z2)                                             (B.166)
```

```
      DIN = SQRTF(DI)                                          (B.167)
      PRINT6, FMAI,FMI                                         (B.168)
      PRINT 7, TINF, RE                                        (B.169)
      PRINT19, BE, X, FMAO, DIN                                (B.170)
      GO TO 54                                                 (B.171)
   21 DEL = SQRTF(Z2)                                          (B.172)
   89 IF(DEL -0.0)90,90,91                                     (B.173)
   90 DUDY = 9.8765                                            (B.174)
      GO TO 99                                                 (B.175)
   91 DUDY = RAT/DEL                                           (B.176)
   99 BE = T*RE*Z2*FK                                          (B.177)
      THE = AA*DEL                                             (B.178)
C     LEADING EDGE VARIATION                                   (B.179)
  601 IF(J-1)403,201,202                                       (B.180)
  201 X = X +0.0001                                            (B.181)
      IF(X-0.001) 15,700,700                                   (B.182)
  202 X = X +0.001                                             (B.183)
  700 CONTINUE                                                 (B.184)
C     DRAG COEFF                                               (B.185)
  120 DET = 0.0                                                (B.186)
      DCD = 0.0                                                (B.187)
      CDM = 0.0                                                (B.188)
      DO 125 IJ = 1,11                                         (B.189)
      FBI = 2.*DET-2.*(DET**3) +DET**4                         (B.190)
      GBI = (DET -3.*(DET**2) +3.*(DET**3)
     -DET**4)/6.                                               (B.191)
      UUJ = FBI +BE*GBI                                        (B.192)
```

```
      DCD = DEL*DET*UO*UUJ*(1.-UO*UUJ)                    (B.193)
      CDM = CDM +DCD                                      (B.194)
  125 DET = DET +0.1                                      (B.195)
      YD = X*(FMU+(FMU**3)/3.+2.*(FMU**5)/15.+17.*
     (FMU**7)/315.)                                       (B.196)
      DY = YD -DEL                                        (B.197)
      IF(DY)104,105,105                                   (B.198)
  104 CFX = CDM                                           (B.199)
      GO TO 106                                           (B.200)
  105 CFX = CDM +DY*(1.-UO)                               (B.201)
  106 CONTINUE                                            (B.202)
      Z1 = Z2                                             (B.203)
C     TEMP PROFILE THRU STM 520                           (B.204)
C     STM 511 IS ADIABATIC WALL CONDITION                 (B.205)
      IF(II-J) 403,510,520                                (B.206)
  510 FH = T                                              (B.207)
  511 FHP = 0.0                                           (B.208)
      ET = 1.0                                            (B.209)
      DET = 0.01                                          (B.210)
      FII = FI                                            (B.211)
      IT = 1                                              (B.212)
      IK = 1                                              (B.213)
      DO 500 IJ = 1,101                                   (B.214)
  503 IF(IK-IJ) 403,504,505                               (B.215)
  504 FHI(I,IT) = FH*FMO                                  (B.216)
      IK = IK +10                                         (B.217)
```

```
      IT = IT +1                                                    (B.218)
  505 CONTINUE                                                      (B.219)
      ET = ET -DET                                                  (B.220)
  703 CONTINUE                                                      (B.221)
      FBE = 2.0*ET -2.0*(ET**3) +ET**4                              (B.222)
      GBE = (ET -3.0*(ET**2) +3.0*(ET**3)
     -ET**4)/6.0                                                    (B.223)
      U = FBE + BE*GBE                                              (B.224)
      FH = 1. +FMA2*(PR**0.5)*GH*(1.-U)                             (B.225)
C     IONIZATION PERCENT                                            (B.226)
      XA = XB                                                       (B.227)
      XB = (E**(QI*(1.-FH)/(BK*TO*TINF)*(FH**2.5)                   (B.228)
      FI = SQRT(XB/(XA*XA*PI +XB) *0.001                            (B.229)
      FMO = FH*(1.-FI) +FH**(5./2.)*FI                              (B.230)
      REI = RE*UO/(FMO*FH)                                          (B.231)
      PRI= PR*FMO/2                                                 (B.232)
      IF( ABSF(PRI-PR) -0.02) 701,701,702                           (B.233)
  702 PR = PRI                                                      (B.234)
      RE = REI                                                      (B.235)
      GO TO 703                                                     (B.236)
  701 CONTINUE                                                      (B.237)
  500 CONTINUE                                                      (B.238)
      II = II +10                                                   (B.239)
      I = I+1                                                       (B.240)
  520 CONTINUE                                                      (B.241)
      C = ABSF(BE)                                                  (B.242)
```

```
      IF(C-12.)300,300,399                                    (B.243)
  300 CONTINUE                                                (B.244)
  399 PRINT6, FMAI,FMI                                        (B.245)
      PRINT 7, TINF, RE                                       (B.246)
      IF(FMAO-1.) 53,53,54                                    (B.247)
   53 PRINT 2, X                                              (B.248)
   54 M = II                                                  (B.249)
      IF(M-60) 51,51,52                                       (B.250)
   51 N = 1                                                   (B.251)
      GO TO 400                                               (B.252)
   52 N = 5                                                   (B.253)
C     X, BETA, MO, B. L. THICKNESS PRINT OUT                  (B.254)
  400 PRINT4                                                  (B.255)
      PRINT5, (XI(K),BEI(K),FMAJ(K),DELI(K),
     K = 1,I,N)                                               (B.256)
      PRINT 140                                               (B.257)
C     INVISCID FLOW PRINT OUT                                 (B.258)
      PRINT 140                                               (B.259)
      PRINT 127                                               (B.260)
      PRINT 128,(XI(K),UOI(K),TOI(K),PII(K),
     ROI(K),K=1,I,N)                                          (B.261)
C     X, THETA, DRAG, SKIN FRICT, PRINT OUT                   (B.262)
      PRINT 140                                               (B.263)
      PRINT 8                                                 (B.264)
      PRINT 9, (XI(K),THEI(K), CFI(K), DUDI(K),
     K = 1,I,N)                                               (B.265)
C     MODIFIED VELOCITY PROFILE PRINT OUT                     (B.266)
```

```
      PRINT 140                                                    (B.267)
  101 PRINT 60, XI(1),XI(26)                                       (B.268)
      PRINT 61                                                     (B.269)
      PRINT 62,(ETI(L),UUI(1,L),ETI(L),UUI(26,L),
     L =1,11)                                                      (B.270)
      IF(I-51)524,102,102                                          (B.271)
  102 PRINT 140                                                    (B.272)
      PRINT 60, XI(51), XI(76)                                     (B.273)
      PRINT 61                                                     (B.274)
      PRINT 62,(ETI(L), UUI(51,L), ETI(L),
     UUI(76,L), L = 1,11)                                          (B.275)
      IF(I-100)524,103,103                                         (B.276)
  103 PRINT 140                                                    (B.277)
      PRINT 60, XI(100), XI(101)                                   (B.278)
      PRINT 61                                                     (B.279)
      PRINT 62,(ETI(L), UUI(100,L), ETI(L),
     UUI(101,L) , L=1,11)                                          (B.280)
  524 CONTINUE                                                     (B.281)
C     MODIFIED TEMP PROFILE PRINT OUT                            (B.282)
      PRINT 140                                                    (B.283)
      PRINT523, XI(1), XI(26), XI(76), XI(101)                     (B.284)
      PRINT 140                                                    (B.285)
      PRINT 521                                                    (B.286)
      PRINT 522, (ETI(L), FHI(1,L), FHI(26,L),
     FHI(76,L), FHI(101,L), L = 1,11)                              (B.287)
  404 IF(AJ-AK)403,403,30                                          (B.288)
  403 STOP                                                         (B.289)
      END                                                          (B.290)
```

SYMBOLS

a	Speed of sound
B	Magnetic flux density
C_d	Coefficient of total drag
C_f	Coefficient of viscous drag (skin friction)
c_p	Specific heat at constant pressure
$\overline{D}$	Displacement vector
E	Defined by equation 4.29
$\overline{E}$	Electric intensity
exp	Natural exponential
$f(\eta)$	Velocity ratio (see equation 6.1)
$F(\eta)$	Component of $f(\eta)$
$G(\eta)$	Component of $f(\eta)$
h	Enthalpy
H	Magnetic intensity
Ha	Hartmann number, $(\sigma B^2 L^2/\mu)^{1/2}$
$\overline{i}, \overline{j}$	Unit vectors
J	Electrical current
k	Boltzman's constant (Chapter II)
k	Coefficient of thermal conductivity
K	Component of β, defined by equation 6.44
K'	Component of β, defined by equation 6.44
L	Length

ln	Natural logarithm
M	Mach number
P	Pressure
Pr	Prandtl number, $\mu c_p/k$
P(x)	Defined by equation 6.61
$\bar{q}$	Velocity vector
Q(x)	Defined by equation 6.62
r_e	Larmor radius
R	Gas constant
Re	Reynolds number, $\rho uL/\mu$
t	Time
T	Temperature (Chapter II)
T	Density ratio at the wall (Chapter VI)
u,v	Components of velocity
x,y	Coordinates
z	δ_1^2/L^2
β	Body shape factor, defined by equation 6.8
γ	Ratio of Specific heats
δ	Boundary layer thickness
δ_1	Momentum boundary layer thickness
δ^*	Defined by equation 6.26
δ_σ	Defined by equation 6.27
ϵ_e	Permittivity
η	Dimensionless coordinate, defined by equation 6.1
θ	Defined by equation 6.25
θ_H	Defined by equation 6.30

θ_σ Defined by equation 6.31

λ Magnetic influence parameter, $\sigma B^2 L/\rho u$

Λ Coefficient of thermal conductivity (Chapter II)

μ Coefficient of viscosity

μ_e Permeability

μ_1 Second coefficient of viscosity

π Constant, 3.141592 . . .

ρ Density

σ Electrical conductivity

τ_w Wall shear

Φ Dissipation function, defined by equation 3.11

Ψ Defined by equation 4.26

Superscripts

$( )^*$ Dimensionless quantity

$( )'$ First derivative with respect to independent variable (exception is K' defined above)

Subscripts

$( )_e$ Inviscid flow variable

$( )_\infty$ Free stream flow variable

Operators

$\frac{\partial}{\partial x}, \frac{\partial}{\partial y}$ Partial derivatives

$\frac{d}{dx}, \frac{d}{dy}$ Total derivatives

$$\frac{D}{Dt} = \frac{\partial}{\partial t} + q \cdot \nabla (\ )$$

$$\nabla = \bar{i}\frac{\partial}{\partial x} + \bar{j}\frac{\partial}{\partial y}$$

Variables appearing in only one section are defined when used.

REFERENCES

1. Bertram, M. H., "An Approximate Method for Determining the Displacement Effects and Viscous Drag of Laminar Boundary Layers in Two-Dimensional Hypersonic Flow," NACA, T.N. 2773, 1952.

2. Bogdonoff, S. M. and A. G. Hammitt, "Fluid Dynamic Effects at Speeds from M 11 to 15," J. of the Aero. Sci., V23, #2, p108, 1956.

3. Braum, Willis H., "Stagnation Boundary Layer with Arbitrary Pressure Gradient," NASA, TND-1703, 1963.

4. Chapman, S., "The Viscosity and Thermal Conductivity of a Completely Ionized Gas," Astrophys. J., V120, #1, p151, 1954.

5. Engel, A. von, Ionized Gases, Oxford Univ. Press, London, 1955.

6. Gilmore, F. R., "Equilibrium Composition and Thermodynamic Properties of Air to 24,000 K," Project RAND, The Rand Corp., RM-1543, 1955.

7. Buganov, D. and I. Poshkarev, "Free Spiraling in Magnetic Fields," Soviet Physics, V7, #6, p480, 1962.

8. Hartmann, J., "Hg-Dynamics I, Theory of the Laminar Flow of an Electrically Conducting Liquid in a Homogeneous Magnetic Field," Det Kgl. Danske Videnskabernes Selskab., V15, #6, p1, 1937.

9. Hartmann, J. and F. Lazarus, "Hg-Dynamics II, Experimental Investigations on the Flow of Mercury in a Homogeneous Magnetic Field," Det Kgl. Danske Videnskabernes Selskab., V15, #7, p1, 1937.

10. Hildebrand, Francis B., Advanced Calculus for Applications, Prentice-Hall, Englewood Cliffs, New Jersey, 1963.

11. Hilsenrath, J. and M. Klein, "Tables of Thermodynamic Properties of Air in Chemical Equilibrium," AEDC, TDR-63-161, 1963.

12. Kaeppeler, H. J. and G. Baumann, "Irreversible Stochastic Thermodynamics and the Transport Phenomena in a Reacting Plasma," Mitteilungen aus dem Forschungsinstitut fur Physik der Strahlantriebe E. V., #8, Stuttgart, 1956.

13. Kantrowitz, A. R. and H. E. Petschek, "An introductory Discussion of Magnetohydrodynamics," Landshoff, R. K., Magnetohydrodynamics, Stanford Univ. Press, Stanford, California, p1, 1957.

14. Kármán, Theodore von and H. S. Tsien, "Boundary Layer in Compressible Fluids," Collected Works of Theodore von Karman, III, 1933-39, Butterworth Scientific Pub., London, 1956.

15. Kármán, Theodore von, From Low Speed Aerodynamics to Astronautics, Pergamon Press, New York, 1963.

16. Lin, S. C., E. L. Resler, and A. Kantrowitz, "Electrical Conductivity of Highly Ionized Argon Produced by Shock Waves," J. of App. Physics, V26, #1, p95, 1955.

17. Lock, R. C., "Stability of the Flow of an Electrically Conducting Fluid Between Parallel Planes Under a Transverse Magnetic Field," Proc. Roy. Soc. A, V233, #1192, p105, 1955.

18. Lysen, J. C. and G. K. Serovy, "The Boundary Layer in a Pressure Gradient," Iowa State University Bulletin, Report No. 43, Ames, Iowa, 1964.

19. Moore, L. L., "A Solution of the Laminar Boundary Layer Equations for a Compressible Fluid with Variable Properties, Including Dissociation," J. of the Aero. Sci., V19, #8, p505, 1952.

20. Rossow, Vernon J., "On Flow of Electrically Conducting Fluids over a Flat Plate in the Presence of a Transverse Magnetic Field," NACA, TN #3971, 1957.

21. Saha, M. N., "Ionization in the Solar Chromosphere," Phil. Mag. and J. of Sci., V40, S6, p472, 1920.

22. Schlichting, Herman, Boundary Layer Theory, McGraw-Hill, New York, 1960.

23. Spitzer, L. Jr. and R. Harm, "Transport Phenomena in a completely Ionized Gas," Phys. Rev., V89, #5, p977, 1953.

24. Stuart, J. T., "On the Stability of Viscous Flow Between Parallel Planes in the Presence of a Coplanar Magnetic Field," Proc. Roy. Soc. A, V221, #1145, p189, 1954.

25. Truitt, Robert W., Hypersonic Aerodynamics, Ronald Press, New York, 1959.

26. Tsien, H. S., "Superaerodynamics, Mechanics of Rarefied Gases," J. of the Aero. Sci., V13, #12, p653, 1946.

27. Williamson, R. R., "On the Equations of State of Ionized Hydrogen," Astrophysical J., V103, #3, p139, 1946.